*Manuscript
Click here to view linked References

The major and trace element glass compositions of the productive Mediterranean volcanic sources: Tools for correlating distal tephra layers in and around Europe

Emma L. Tomlinson[1*], Victoria C. Smith[2], Paul G. Albert[2], Erkan Aydar[3], Lucia Civetta[4], Raffaello Cioni[5], Evren Çubukçu[3], Ralf Gertisser[6], Roberto Isaia[7], Martin A. Menzies[8], Giovanni Orsi[9,10], Mauro Rosi[11], Giovanni Zanchetta[11]

*corresponding author: email: tomlinse@tcd.ie; tel: +353 1 8963856

[1]Department of Geology, Trinity College Dublin, Dublin, Ireland

[2]Research Laboratory for Archaeology and the History of Art, University of Oxford, Oxford, UK

[3] Department of Geological Engineering, Hacettepe University, Ankara, Turkey

[4]Instituto Nazionale di Geofisica e Vulcanologia, Sezione di Napoli-Osservatorio Vesuviano, Napoli, Italy.

[5]Department of Earth Sciences, Università degli Studi di Firenze, Firenze, Italy

[6]School of Physical and Geographical Sciences, Keele University, Keele, UK

[7]Istituto Nazionale di Geofisica e Vulcanologia, Osservatorio Vesuviano, Napoli, Italy

[8]Department of Earth Sciences, Royal Holloway University of London, Egham, UK

[9]Dipartimento di Scienze della Terra, dell'Ambiente e delle Risorse, Università degli Studi di Napoli Federico II, Naples, Italy

[11]Dipartimento di Fisica "E. R. Caianiello", Università degli Studi di Salerno, Fisciano, SA, Italy

[11]Dipartimento di Scienze della Terra, Università di Pisa, Pisa, Italy

Abstract: The increasing application of cryptotephra studies is leading the identification of new tephra marker layers the sources of which in many cases may not be known or may be ambiguous. In this contribution, we discuss the controls on tephra geochemistry in the context of establishing the provenance of an unknown tephra layer. We use the RESET database (https://c14.arch.ox.ac.uk), which contains major and trace element data for a number of European silicic tephra erupted in the period 100 ka to ca. 10 ka, to define new and modify existing tectonic setting discrimination diagrams for use with volcanic glass analyses. Bivariate plots of the elements Rb, Nb, Ta, Y and Th and K_2O, SiO_2, FeO and MgO can be used to identify tephra from different tectonic settings. New, detailed glass chemistry shows that tephra from the productive Neapolitan volcanic centres, Somma-Vesuvius (22-4 ka activity), Campi Flegrei (60-15 ka) and Ischia (75-20 ka), can be separated using major elements, CaO–SiO_2, Na_2O/K_2O-CaO and CaO-MgO. In each of these centres, the tephrostratigraphic record is characterized by the repeated occurrence of similar glass compositions, punctuated by significant changes in magma chemistry. The glass compositions of successive eruptions from Campi Flegrei are similar but there is a significant change in the composition following the Campanian Ignimbrite, and there are comparable compositional changes at Ischia following the Monte Epomeo Green Tuff eruption and at Somma-Vesuvius following the Verdoline event. Distinguishing different tephras from a single volcanic centres is more problematic, and in some instances even impossible, without good chronological and stratigraphic control and/or high-resolution trace element glass data. At Somma-Vesuvius certain major elements can be used to separate glasses from the major chronological phases (Group 1 - Pomici di Base and Verdoline; Group 2 - Mercato and Avellino), but separating tephras within a single group on the basis of glass composition can be problematic.

Key words: tephra, tephrochronology, discrimination diagrams, major and trace element, Neapolitan, Somma-Vesuvius.

1. Introduction

Tephra layers provide isochronous markers in the stratigraphic record and are therefore a fundamental tool for correlating between archaeological, lacustrine, peat and marine archives (tephrostratigraphy e.g. Froese et al., 2008; Lowe et al., 2008a; 2008b; Lowe et al., 2012). In addition, if the precise age of the tephra is known from an independent numerical dating method, then tephra horizons provide age markers within the stratigraphy (tephrochronology). Tephrochronology has a wide variety of applications in palaeoclimatology and archaeology, for example in refining age models in paleoenvironmental records (e.g. Turney et al., 2004; Lowe et al., 2008b; Lane et al., 2013a), the synchronization of those records in order to determine leads and lags of rapid climate changes (e.g. Turney et al., 2004, Davies et al., 2012, Lane et al., 2013b) and interpretation of the relationship between abrupt climate changes and human evolution (e.g. Santacroce et al. 2008; Giaccio et al., 2008; Lowe et al., 2012).

Traditional tephrochronology refers to tephra layers that are visible to the naked eye. More recently, non-visible tephra deposits, termed "cryptotephras" have been identified (e.g. Dugmore et al., 1995). Cryptotephras can be detected in sediment sequences far beyond the range of visible tephra records, greatly expanding the geographic footprint of a given tephra, for example cryptotephras have been identified in ultra-distal localities as far as 7000 km away from the source (Pyle-O'Donnell et al., 2012). This increases the likelihood of the superposition of tephra layers from different source regions at a single location, allowing regional tephrochronologies to be linked (e.g. Lane et al., 2011). However, far-travelled tephras also increases the number of potential sources that may contribute tephra to a given locality. Indeed, new tephras have been discovered that presently are known only as cryptotephra horizons, their proximal equivalents not having been established (Davies et al., 2004; Wutke et al., this volume), these may be from more distant sources and/or may represent smaller eruptions from proximal and medial sources. One critical difference between visible and cryptotephra layers is the number of shards available for analysis: cryptotephras are commonly represented by low shard concentrations (few shards per gram of dry sediment) and may not preserve the full compositional range erupted. Furthermore, the cryptotephra are typically ultra-distal deposits identified by extracting the glass shards from other material using density separation techniques so there is no information on lithics or phenocrysts associated with the glass shards. Major element compositions of the glass shards is the most widely employed method to robustly correlate tephra layers to particular eruptions but the compositions of tephra layers from the same volcano are often very similar (e.g., Smith et al., 2011a; 2011b, Tomlinson et al., 2012). More recently, trace element abundances and ratios of single glass shards have been used as additional discriminators to increase the confidence in proposed proximal-distal or distal-distal tephra correlations (e.g. Albert et al., in press).

Given the number of potential volcanic sources and eruptions recorded as cryptotephra in distal settings, there is a need for comparable data for potential source eruptions in proximal settings in order to establish robust proximal-distal correlations. To this end, we present major and trace element micron-beam glass data for proximal tephra deposits produced during major explosive eruptions of volcanoes in the central and western Mediterranean in the last ~100 kyrs; including deposits from Somma-Vesuvius and Pantelleria (Italy), Santorini (Aegean arc, Greece), Gölcük (western Anatolia, Turkey), Acıgöl and Erciyes Dagi (central Anatolia, Turkey) and Terceira (Azores, Portugal). These data are compared to published major and trace element glass data for volcanoes in Italy (Campi Flegrei, Ischia, Colli Albani, Mount Etna), Greece (Nisyros) and Iceland (Katla, Tindfjallajokull) to demonstrate the importance of micron-beam glass data for proximal-distal tephra correlations.

The dataset of proximal tephra geochemistries was collected for the NERC RESET project (RESponse of humans to abrupt Environmental Transitions) and includes data for most of the large explosive eruptions in Europe between 3 and 100 ka. The central and western Mediterranean area is an ideal location for the application of tephrochronology because of the presence of a large number of highly explosive and frequently active volcanoes (Fig. 1). These volcanoes occur in a range of geodynamic settings, leading to a range of magma chemistries. These geochemical signatures imparted at different tectonic settings allow the provenance of an unknown glass shard to be easily established yet they are not routinely used by tephrochronologists. Here we clearly show the compositions that are characteristic of different volcanoes over Europe. This paper also demonstrates that detailed major and trace element chemistry can be used to distinguish between tephra layers from successive eruptions from the same source, using eruptions from Ischia, Campi Flegrei and Somma-Vesuvius as examples. We also focus on the diagnostic features of tephra deposits erupted from Somma-Vesuvius between 4 and 22 ka.

2. Geochemical dataset

Major and trace element micron-beam glass data was collected using a wavelength-dispersive electron microprobe (WDS-EMPA) and Laser Ablation Inductively Couple Plasma Mass Spectrometry (LA-ICP-MS), respectively, using the methods outlined in supplementary file S1. The full dataset is available in supplementary file S2.

All data for glass shards are obtained by micro-analytical techniques. Proximal-distal tephra correlations require micron-scale glass (and/or mineral) analyses. Bulk-rock analyses of tephra deposits cannot be used for proximal-distal correlations as the samples include crystals and the crystal proportion decreases with distance from the vent, thus analysis from deposits at different distances from the vent are not directly comparable. Furthermore, even if glass separates are obtained the difference in analytical scale may introduce systematic differences and/or differences in the degree of apparent heterogeneity in the composition of a tephra population. Thus, proximal major and trace element datasets of volcanic glasses, such as presented here, represent an important tool for using tephra as stratigraphic and chronological markers in sedimentary successions

The influence of phenocrysts on the whole-rock composition is particularly evident in the Lower and Upper Pumice eruption deposits from Nisyros (Greece). The different eruption deposits contain 5-10 vol.% and 15-20 vol.% crystals, respectively (Tomlinson et al., 2012a). Figure 2a shows that: 1) the glass is depleted relative to the whole-rock data in elements that are compatible in the main phenocryst phases of plagioclase (Na_2O, Sr), clinopyroxene (MgO, FeO, CaO, V), Fe–Ti oxides and zircon, while the incompatible elements are proportionally enriched in the glass data; and 2) the effect is more marked at higher phenocryst contents. This clearly shows that whole-rock data of volcanic samples containing crystals are offset from glass data of the same deposits.

Microlites (small crystals; Fig. 2b) also introduce compositional heterogeneity that is not present in whole-rock data. This is demonstrated in figure 2 c-d, where we compare whole-rock (ICP-AES and ICP-MS) and micron-beam (EMPA-WDS and LA-ICP-MS) glass data for the two samples from the Pomici di Base eruption of Somma-Vesuvius: SM21 is microlite-rich with numerous, small (30-60 μm) biotite and plagioclase crystals, while SM28 is microlite-poor. The micron-beam glass data for SM28 shows a greater degree of scatter than sample SM21 across all elements (Fig. 2c). Trace element heterogeneity is less marked, with no real difference apparent between the microlite-rich and microlite-poor sample (Fig. 2d), this reflects the larger beam diameter required for trace element analyses (25 to 34 μm) relative to major element analyses (5 to 10 μm) which has the effect of homogenising the glass and microlites and thus leads to systematic errors, such as tending to higher Sr when plagioclase microlites are analysed.

Analytical scatter introduces apparent heterogeneity to low concentration elements in glass datasets. During repeat analysis of the MPI-DING glass standards, the relative standard deviation (100 x standard deviation / average) is above 10% at concentrations below ~0.6 wt% in WDS-EMPA major element data and below ~3 ppm in LA-ICP-MS trace element data (Fig. 2e-f)[1]. In intermediate and silicic volcanic glasses, affected elements typically include TiO_2, MnO and P_2O_5 (WDS-EMPA) and the trace elements such as the middle to heavy rare earth elements (LA-ICP-MS); therefore these should be treated with caution when making tephra correlations

3. Geochemical identification of tectonic setting

For the purposes of this study, we recognise three principal tectonic settings for explosive volcanism in Europe:

- Subduction of oceanic plates beneath continental lithosphere.
- Post-subduction settings in which the mantle melts are influenced by subduction fluids from a previous period of active subduction.
- Anorogenic magmatism in extension-related or intraplate hot spot

[1] It should be noted that the exact concentration at which precision deteriorates depends on the spot size (both methods) and on wave intensity (EMPA-WDS) or isotope abundance and sensitivity (LA-ICP-MS).

settings.

The geographical distribution and geodynamic settings of the studied volcanoes, as constrained by primitive magma compositions and geophysical observations, are shown in Figure 1 and summarised in Table 1. We focus on eruptions in the central and eastern Mediterranean, however data for volcanic sources in Iceland (Tomlinson et al., 2010, 2012) and the Azores (this study) are given as examples of anorogenic magmatism. Below, we use our dataset to review the geochemical characteristics of intermediate and silicic glass shards produced in different tectonic settings. We then use this data to define discrimination diagrams that allow the tectonic setting and the source volcano to be determined. These plots are of particular use in the identification of ultra-distal tephra, for example, establishing the source of a cryptotephra found in a cave in Morocco as anorogenic and from the Azores (Barton et al., this volume).

3.1 Tectonic setting

3.1.1 Subduction settings (Aeolian Islands, Aegean arc, Central Anatolia)

Tephra erupted from volcanoes in active or recent subduction settings (Table 1; Fig. 3a), the latter being where the downgoing plate is still present below the volcanic centres, have subalkaline (Le Maitre, 1989) medium- to high-K compositions, and range from calc-alkaline basaltic andesite to rhyolite melts.. These subduction-related magmas are also characterized by higher concentrations of CaO, MgO and FeO and lower alkalis for a given SiO_2 (Fig. 3c-e) with low K_2O/Na_2O (typically <1.0).

Subduction-related magmas have distinctive trace element fingerprints, a result of fluid involvement in their genesis. They are enriched in fluid mobile Large Ion Lithophile elements (LILE e.g. Rb, Ba, K; Tatsumi et al., 1986) relative to insoluble high field strength elements (HFSE, e.g. Nb, Ta, P, Ti, and the Rare Earth Elements (REE) La to Lu) (Gill 1981; Pearce 1982; Ellam and Hawkesworth 1988, Hawksworth et al., 1994; Pearce and Peate 1995). Thorium may be enriched by the addition of sediment to the mantle during subduction or by interaction of mantle derived magma with continental crust. Thus, subduction-related tephra from the Aegean, Aeolian and central Anatolian arcs show large negative anomalies in Nb, Ta and Ti, low REE concentrations and enrichment in Rb, Th and U on mantle-normalised trace element plots (Fig. 3f) and thus have high LILE/HFSE and LILE/REE ratios.

3.1.2 Post-subduction settings (Neapolitan volcanic area, Roman Province, Western Anatolia)

Tephra from post-subduction settings in the Roman (Latium) Province (Italy) and Western Anatolia (Turkey) (Fig. 3a) belong to the shoshonite-latite association and are trachytic to foiditic. These tephras are characterized by high K_2O/Na_2O (>0.4, dominantly 1-3) and low TiO_2 <0.75 wt%, with dominantly metaluminous ($Na_2O+K_2O < Al_2O_3 < Na_2O+K_2O+CaO$) compositions. These tephras have subduction-related trace element compositions with elevated Th, U and Rb and negative anomalies in Nb and Ta. However, the depletions in Nb and Ta are less extreme in post-subduction relative to active subduction settings, thus Nb to Zr abundances of post-subduction tephra are more elevated than in tephra from volcanoes experiencing active subduction and overlap with those of anorogenic tephra on mantle-normalised trace element plots (Fig. 3f). It should be noted that tephra produced from the Aeolian island volcanoes (Italy) in the last 100 kyrs typically show these post-subduction characteristics even though they are in an actively subducting environment. , However, glasses with active subduction characteristics were erupted at Lipari (e.g. Monte Pilato tephra) and Salina (e.g. Lower Pollara pyroclastics) (Albert, 2012).

3.1.3 Anorogenic settings (Azores, Iceland, Pantelleria, and Etna)

High-K trachytes and trachy-rhyolites (Fig. 3a) with K_2O/Na_2O <1 are typically erupted in intraplate settings (e.g. Wilson and Bianchini, 1999) at the Azores (Portuguese islands), Pantelleria (Italian island) and Sicily (Italy). Tephra from the Azores and Pantelleria are peralkaline ($Na_2O+K_2O > Al_2O_3$) trachy-rhyolites with low CaO (<1 wt%), MgO (<0.35 wt%) and high FeO (>4.3 wt%) contents that do not vary with SiO_2 (Fig. 3c-e). The anorogenic tephra show approximately equal levels of enrichment in Rb, Th, U, Ta and Nb, which is attributed to derivation from an enriched mantle without significant crustal involvement. Tephras from these locations have elevated Y, Th and HREE contents and lack negative anomalies in Nb and Ta, they also show lower levels of enrichment in soluble LILE elements (K, Rb) relative to subduction-related tephra (Fig. 3f), consistent with melt rather than fluid transport of the incompatible elements.

In contrast to Pantelleria, tephras erupted from Etna (Sicily) are metaluminous with higher CaO and MgO; TiO_2 is also significantly higher in Etna tephra deposits. Etna glasses do not show equal levels of enrichment in Rb, Th, U, Ta and Nb. Instead, Th and U are slightly enriched, and Nb and Middle Rare Earth

Elements (MREE) are depleted, suggesting some crustal involvement in magma genesis.

3.2 Discriminating tephra from different tectonic and volcanic sources

It is clear from the above discussion that K, Rb, Nb, Ta, Y and Th are the most useful elements for the identification of the tectonic setting and source of silicic tephra around the Mediterranean. These relative concentrations relate to the source compositions and crystallization histories that prevail at the different volcanoes.

3.2.1 Subduction-related versus anorogenic tephra

Anorogenic silicic tephra are medium to high-K alkaline and do not extend into the shoshonite-latite field. The most significant differences between European silicic tephra from subduction related (active and post) and anorogenic settings is the elevated Th and U and depleted Nb and Ta of subduction-related glasses relative to anorogenic glasses. Plots of Nb vs Th and Ta vs U (or those same elements normalized to Rb to account for varying degrees of fractionation) clearly discriminate between silicic tephra from subduction-related and anorogenic settings (Fig. 4a,b), although Etnean tephras straddle the boundary between the two fields. These plots are similar to the basalt discrimination diagrams of Wilson and Bianchini (1999).

3.2.2 Active versus post subduction tephra

Pearce et al. (1984) used Rb, Nb and Y to define trace element discrimination diagrams for plutonic rocks (specifically granite) from different tectonic settings.

We have modified these diagrams to account for the fact that glasses in volcanic rocks are more evolved, and so extend to higher absolute incompatible element concentrations than their whole-rock plutonic equivalents (Fig. 4e). Thus, the empirical boundaries defined by the European tephra in this study are shifted to slightly higher values relative to the granite diagrams of Pearce et al. (1984). There is reasonable separation and minimal overlap of tephra from active subduction, post subduction and anorogenic settings in a diagram of Rb versus (Y+Nb). Tephra from volcanoes in active- and post-subduction settings can also be separated on a plot of Nb/Rb vs Ta/Rb (Fig. 4f), where the use of Rb as a denominator minimises the effect of variable degrees of crystal fractionation.

Tephra from volcanoes in active and post subduction settings can be distinguished on the basis of major element composition. Post-subduction tephra typically have higher FeO/(FeO+MgO) for a given SiO_2, (Fig. 4d) than tephra from active subduction settings, although there is significant variation within individual arcs. Post-subduction tephra are also more K-rich, extending into the shoshonite-latite-foidite-phonolite field, while tephra from active subduction zones are dominantly medium to high-K alkaline in composition (Fig. 4c).

4. Distinguishing different volcanic sources in the same region

As an example of distinguishing between tephra from different volcanic sources within a region, we discuss use those in the Neapolitan volcanic area, Campania, Italy. The still active volcanoes in this area (Somma-Vesuvius, Ischia, and Campi Flegrei) have been frequently active in the last 100 kyrs and are source of widespread tephras in the Mediterranean. The annually laminated Lago Grande di Monticchio sedimentary archive preserves 345 primary tephra layers, dominantly sourced from the these volcanoes, of which 30 have been precisely correlated with dated volcanic events (Wutke et al., this volume). The uncorrelated tephra layers highlight the need for robust source discriminants that take into account the full geochemical range exhibited by a source.

Proximal volcanic deposits of volcanoes around the world demonstrate that individual silicic volcanic sources are often characterized by the repeated eruption of similar magma compositions (e.g. Pabst et al., 2008; Smith et al., 2011a). These volcanoes are also known to periodically experience significant shifts in composition after a very large eruption, which may reflect a major change in the composition of the parental magma and/or magma storage conditions. This is seen at Campi Flegrei following the Campanian Ignimbrite eruption (Pappalardo et al 1999, D'Antonio et al., 2007; Pabst et al., 2008; Arienzo et al., 2009; Di Renzo et al., 2011; Tomlinson et al., 2012), at Ischia following the eruption of the Monte Epomeo Green Tuff (Civetta et al., 1991; Piochi et al., 1999; Brown et al., 2014, Tomlinson et al., accepted), and at other silicic volcanoes following caldera-forming events (e.g., Taupo Volcanic Zone, New Zealand; Smith et al., 2005). These large events provide critical markers within detailed tephrostratigraphic records as they are widespread and denote the change in magma composition. A detailed record of the temporal changes in composition is invaluable for identifying the volcanic source and an approximate age of an uncorrelated tephra.

4.1 Neapolitan volcanic area

The Neapolitan Volcanic Area comprises the active volcanoes of Somma-Vesuvius, Campi Flegrei and Ischia that surround the city of Naples (Orsi et al., 2003; Santacroce et al., 2003). The island of Ischia is the most westerly of the Neapolitan volcanoes, and is thought to represent the remnants of a larger volcano (Orsi et al., 1999; Bruno et al., 2002). The current volcanic field is the result of dominantly magmatic and phreatomagmatic explosive activity dating back over 150 kyrs and includes at least one caldera collapse attributed to the 55 ka (Watts et al., 1996) Monte Epomeo Green Tuff eruption (MEGT; Buchner, 1986; Vezzoli, 1988, Civetta et al., 1991, Orsi et al., 1991; Brown et al., 2008). Tephra from Ischia is phono-trachytic to trachytic and latitic in composition (e.g. Civetta et al., 1991), with phenocrysts of plagioclase, clinopyroxene, alkali-feldspar, biotite and Fe-Ti oxides.

Campi Flegrei volcano is located on the same NE-SW fault system as Ischia. The volcano comprises two nested calderas formed during the 39 ka (De Vivo et al., 2001) Campanian Ignimbrite (CI) and the ~15 ka (Deino et al., 2001) Neapolitan Yellow Tuff (NYT) eruptions (Orsi et al., 1996). Volcanic deposits found in and directly around the caldera record the activity of the last ~60 ka (Pappalardo et al., 1999), and deposits on the Campanian Plain that are most likely from Campi Flegrei suggest that activity dates back to 290 ka (Rolandi et al, 2003). Campi Flegrei has been very productive since the NYT, with more than 70 eruptions in the last 15 kyrs (Di Vito et al., 1999; Orsi et al., 2004; Smith et al., 2011b; Selva et al., 2012; Capuano et al., 2013). Tephra from Campi Flegrei is dominantly trachyte to phonolite (D'Antonio et al., 2007; Pabst et al., 2008; Arienzo et al., 2009, 2010; Di Renzo et al., 2011; Smith et al., 2011b, Tomlinson et al., 2012b), and contains phenocrysts of alkali feldspar, minor clinopyroxene, biotite, plagioclase, Fe-Ti oxides and rare amphibole.

Somma-Vesuvius is a stratovolcano located southeast of Naples city. It is comprised an old cone (Monte Somma), repeatedly dissected following the four main plinian eruptions of this volcano, and the young cone (Vesuvius) that grew in the summit caldera after the AD1631 eruption. The volcanic area has been active since 300 ka (Brocchini et al., 2001), effusive activity was dominant during the growth of Monte Somma (ca. 39-22 ka) and activity has been more explosive in the last 22 ka with four Plinian and at least 7 sub-Plinian eruptions (Di Renzo et al., 2007; Cioni et al., 2008; Santacroce et al., 2008). Tephra associated with these explosive eruptions typically ranges from latite-trachyte to phonolite and tephriphonolite (Joron et al., 1987; Ayuso et al., 1998), with phenocrysts of sanidine, plagioclase, clinopyroxene and Fe-Ti oxides. Young (post AP3) pyroclastic products have leucite phenocrysts, which are particularly dominant in the AD79 and post-AD79 deposits (Ayuso et al., 1998).

4.2 Compositions of tephra from the Neapolitan volcanoes

This discussion includes major and trace element glass compositions of tephra from Campi Flegrei (TLa, TLc, TLf, CI, TLo, PRa, VRa, VRb, NYT, Pomici Principali, Agnano Monte Spina) and Ischia (Sant'Angelo tephra, Olummo, Tisichiello, Porticello, MEGT, Schiappone, Pietre Rosse, Agnone) that are published in Smith et al., (2011b), Tomlinson et al., (2012b), and Tomlinson et al., (accepted). Data for younger Ischia samples (St Montano and the younger Sant'Angelo tephra) and for Somma-Vesuvius tephra (Pomici di Base, Verdoline, Mercato, Avellino) are from this study.

Silicic tephra produced during explosive eruptions at Somma-Vesuvius, Campi Flegrei and Ischia over the last <80 ky show considerable geochemical overlap (Fig. 5a) but the sources can be identified - Table 3 summarises the most useful plots for discriminating between these three sources. The most useful major element plots are CaO–SiO_2, Na_2O/K_2O-CaO and CaO-MgO (Fig. 5), these separate silicic tephra from Ischia, Campi Flegrei and Somma-Vesuvius with only minimal overlap. The most useful trace element plots are Sr-Zr or Zr/Sr-Zr, and various inter-element plots of Y, Zr, Nb, Th and Ta (Fig. 6).

4.2.1 Campi Flegrei (60-12 ka)

Glasses produced during explosive eruptions of Campi Flegrei straddle the phonolite-trachyte boundary (Fig. 5a). Tephra compositions are highly variable, however two trends are apparent:

- Older, Pre-CI and CI tephra (60-39 ka) – These glasses are characterized by low CaO (Fig. 5b) and show slightly decreasing CaO, FeO and Al_2O_3 with increasing SiO_2; the ratio Na_2O/K_2O is typically 0.79 ± 0.34 (0.3 to 1.1). Pre-CI and CI tephra are moderately to highly evolved with Zr/Sr = 5-84 (Fig. 6a) and the ratio Zr/Th is constant (13 ± 1; Fig. 6d) as are ratios of HFSE to Th (Nb/Th = 2.4 ± 0.3; Ta/Th = 0.11 ± 0.01; Tomlinson et al., 2012b).

- Younger, Post CI tephra (≥15 ka) – These glasses have higher CaO, MgO, K_2O, V and lower Na_2O than older Campi Flegrei tephra and show decreasing CaO (Fig. 5b), MgO, FeO and TiO_2 and increasing Na_2O with increasing SiO_2; the ratio Na_2O/K_2O is lower at to 0.46 ± 0.20 (0.3 to 1.0). Relative to Pre-CI tephra, Post-CI tephra are less evolved, with Zr/Sr typically 0.7-7 (Fig. 6a), while ratios of Zr/Th (10.7 ± 1.3; Fig. 6d) and HFSE to Th (Nb/Th = 1.75 ± 0.15; Ta/Th = 0.08 ± 0.01; Tomlinson et al., 2012b) are lower than in the older Pre-CI/CI tephra.

Campi Flegrei glasses show minor overlap with tephras from Ischia: Pre-CI/CI glasses with low CaO concentrations (CaO < 1.8 wt%) partially overlap with Ischia glasses on all major and trace element plots and so care must be taken when considering tephra older than 39 ka. Post-CI tephra are characterized by higher CaO and MgO and are clearly distinct from Ischia tephra (Fig. 5 b-d). Overall, Campi Flegrei glasses are most clearly separated from Ischia tephra on plots of SiO_2 ‘vs’ CaO (Fig. 5b), Na_2O/K_2O ‘vs’ CaO (Fig. 5c) and Zr/Sr ‘vs’ Th, while Y ‘vs’ Th (Fig. 6c) provides additional constraints.

Campi Flegrei tephra show partial overlap with group 1 Somma-Vesuvius glasses and significant overlap with group 2 Somma-Vesuvius glasses in most major and trace elements. This is mainly a consideration for the post-CI tephra, which overlap with the group 1 Somma-Vesuvius glasses in age as well as chemistry. However, Campi Flegrei glasses are clearly separated from Somma-Vesuvius tephra on a plot of CaO ‘vs’ MgO (Fig. 5d), while additional constraints are provided by a plot of Ta/Th ‘vs’ Nb/Th (Fig. 6b).

4.2.2 Ischia (75-20 ka)

Volcanic glasses produced during explosive eruptions from Ischia straddle the phonolite-trachyte boundary (Fig. 5a). Proximal glasses from Ischia are characterized by low CaO (typically <1.5 wt%) and high Na_2O (>5.6 wt%) giving high Na_2O/K_2O ratios (0.7-1.5) (Brown et al., 2008, 2014; Tomlinson et al., accepted), they show a trend of decreasing Na_2O and FeO decrease with increasing K_2O and SiO_2, while MgO and CaO compositions remain fairly constant (Fig 6. b,d). The studied Ischia glasses have a wide range of incompatible trace element concentrations extending to highly enriched concentrations (Zr 160-1110 ppm; Tomlinson et al., accepted) and are characterized by high Zr/Sr ratios (up to 670; Fig. 6a).

Ischia glasses show minor overlap with Pre-CI/CI tephra at the high CaO and low Na_2O end of the range (CaO > 1.5 wt%; Fig. 5 b,c), however they can be distinguished on a plot of Zr/Sr 'vs' Th (Fig. 6a). Furthermore, the Ischia glasses show lower degrees of incompatible element enrichment and sit on trends of higher Y, Zr, Nb and Ta for a given Th (e.g. Fig. 5 c,d) than the pre-CI/CI tephra. Ischia tephra are clearly distinguished from tephra from Somma-Vesuvius on most major (e.g. CaO 'vs' SiO_2 and MgO 'vs' CaO; Fig. 5b,d) and trace element plots (e.g. Zr/Sr 'vs' Th; Fig 7a).

4.2.3 Somma-Vesuvius (22-4 ka)

Glasses produced during explosive eruptions of Somma-Vesuvius vary from basaltic trachyandesite to trachyte and extend into the tephriphonolite and phonolite fields (Fig. 5a). Two trends are defined for this time period:

- Group 1 or B-M interval (Santacroce et al., 2008) includes the explosive eruptions of Pomici di Base and Verdoline. These glasses show a trend of decreasing CaO, FeO and MgO with increasing SiO_2 (Fig. 5b,d) and constant K_2O and Na_2O with low Na_2O/K_2O (0.3 to 0.7; Fig. 5c). Group 1 glasses have low incompatible element contents (Zr 170-380 ppm) and low Zr/Sr (<1.2; Fig. 6a) but high ratios of Ta/Th (Fig. 6b).
- Group 2 or the M-A interval (Santacroce et al., 2008) includes the explosive eruptions of Mercato and Avellino. These glasses have low CaO, FeO and MgO concentrations (typically less than 3.2 wt%, 2.7 wt% and 0.35 wt%, respectively) for a range of SiO_2 contents (Fig. 5b,c). In contrast, Na_2O and K_2O show significant variability, with Na_2O/K_2O ranging from 0.5 to 1.5. Group 2 glasses have high Zr contents (275 - 815 ppm relative to group 1 and glasses, giving moderate values of Zr/Sr (up to 65; Fig. 6a). The group 2 glasses have high Th contents relative to the group 1 products, and thus sit on a distinct trend of lower Ta/Th (Fig. 6b).

Tephra from Somma-Vesuvius can be clearly distinguished from Ischia tephra on a variety of major element plots (Fig. 5). Somma-Vesuvius glasses show significant overlap with Campi Flegrei glasses in both major and trace element composition, in particular the Post-CI glasses, which also overlap in age. However, Somma-Vesuvius glasses can be clearly distinguished on the basis of higher CaO for a given MgO (Fig. 5d), while additional constraints are provided by plotting Ta/Th vs. Nb/Th (Fig. 6b).

5. Distinguishing between tephra from a single source: Somma-Vesuvius (22-4 ka)

In this section, we discuss the separation of tephras produced at a single source using Somma-Vesuvius as an example. Joron et al., (1987) and Ayuso et al. (1998) sub-divided the Somma-Vesuvius products into three groups on the basis of silica saturation and phenocryst mineralogy. Group 1 magmas are older than the ~8.5 ka Mercato tephra and are silica saturated to slightly SiO_2-undersaturated. Group 2 magmas are mildly silica undersaturated, they span the period from Mercato to A.D. 79 and include the Avellino and at least six other smaller explosive eruptions (Andronico and Cioni, 2002). A detailed review of the age and lithological features of the major explosive eruptions of Somma-Vesuvius is given in Santacroce et al., (2008) and Cioni et al. (2008).

In this work, we have analysed proximal tephra produced by VEI 4 and VEI 5 eruptions of Somma-Vesuvius during chronological Group 1 (pre-18 ka) and Group 2 (post-10 ka) eruptions (Table 2). Group 1 includes: the 22 ka Pomici di Base eruption, also known as "Basal", "Pomici Basali" and "Sarno" (Capaldi et al., 1985, Arno et al., 1987 and Landi et al., 1999), and the 19 ka Verdoline eruption, also known as "Greenish Pumice" and "Novelle Seggiari Bosco" (Santacroce et al., 2008, Cioni et al., 2003, Ayuso et al., 1998). The ~8.5 ka Mercato and the ~3.9 ka Avellino eruptions (Sevink et al., 2011; Zanchetta et al., 2011) form Group 2. The data is summarized in Table 2, and the full glass chemistry dataset is available in supplementary information (S3).

Whole-rock major and trace element data is available for the Vesuvius eruptions studied here (e.g. Ayuso et al., 1998; Santacroce et al., 2008), and there is some major element glass data for the younger products (Santacroce et al., 2008; Turney et al., 2008). Santacroce et al. (2008) reviewed the available data for the purposes of tephrochronology and showed that, while the different Somma-Vesuvius groups can be separated using major and trace element whole-rock data, there is significant geochemical overlap between tephra within a single group. Here we present detailed major and trace element composition of individual glass shards for the major eruptions in the last 36 ka to outline geochemical discriminators for the various eruptions. These geochemical discriminators are particularly important in cryptotephra studies, where the lithic and phenocryst phases, that are characteristic of the Vesuvius products, are absent and thus cannot be used to aid tephra identification.

5.1 Studied eruptions from Somma-Vesuvius

The Somma-Vesuvius eruptions studied here display considerable compositional variability, previously also noted by Santacroce et al., (2008). Given that the full range of compositions may not be recorded in the distal cryptotephra horizons, care must be taken when trying to identify the particular eruption using the glass compositions.

5.1.1 Pomici di Base glasses span a wide compositional range from latite to trachyte, overlapping extensively with both Codola and Verdoline glasses in major element composition and extending to less evolved compositions, with CaO 2.9 – 10.6 wt% (Fig. 7c). Concentrations of MgO and FeO decrease linearly with decreasing CaO, while Na_2O, K_2O and SiO_2 increase (Fig. 7). Pomici di Base glasses have Th/Zr = 0.083 ± 0.007, Nb/Zr = 0.15 ± 0.01 and Ta/Zr = 0.0078 ± 0.0006 (Fig. 8). The least evolved Pomici di Base glasses sit on a trend of high REE to Zr, at intermediate incompatible element concentrations the glasses switch to a trend of lower REE relative to Zr forming a sub-parellel trend (Fig. 8).

5.1.2 Verdoline glasses are trachytic and form a fairly tight compositional range (58.8 - 60.9 wt%; SiO_2; 2.5 - 4.3 wt% CaO; Fig. 7c) that is partially overlapped by the most evolved Pomici di Base tephra in major element composition. Verdoline glasses sit on the same Nb-Zr and Ta-Zr trends as Pomici di Base with Th/Zr = 0.090 ± 0.006, Nb/Zr = 0.16 ± 0.01; Ta/Zr = 0.0087 ± 0.0006 and sit on the trend of low REE/Zr defined by the least evolved Pomici di Base glasses (Fig. 8). However absolute concentrations of incompatible elements are higher in the Verdoline glasses (Zr > 239 ppm; Nb > 49 ppm; Th > 21 ppm) than in Pomici di Base glasses.

5.1.3 Mercato glasses are phonolitic and are the most evolved of the studied 22-4 ka Somma-Vesuvius tephra units, extending to the lowest CaO, FeO and MgO values observed (Fig. 7a-c). The Mercato glasses show only limited geochemical variability, extending to higher Na_2O and lower Al_2O_3 and K_2O with decreasing CaO (Fig. 7). Mercato glasses have the highest incompatible element concentrations of the studied glasses (Zr > 289 ppm; Nb > 66 ppm and Th > 30 ppm; Fig. 8). The ratio Th/Zr = 0.11 ± 0.02, but ratios of Nb/Zr, Ta/Zr and Ce/Zr are lower than observed in phase 1 and form distinct trends on trace element biplots (Nb/Zr = 0.15 ± 0.06).

5.1.4 Avellino glasses comprise two populations, phonolite and tephri-phonolite. The phonolite population overlaps extensively with the Mercato tephra compositions, being characterized by low CaO, FeO and MgO and extending to high Na_2O (Fig. 7). However, the tephra-phonolite population is distinct, lying at lower SiO_2 (55.8 ± 0.6 wt%) and higher Na_2O. However, Avellino glasses have higher higher Nb/Zr and Ta/Zr (Fig. 8) and form trends that are sub-parallel to, rather than directly overlapping those of Mercato glasses.

5.2 Discriminating Somma-Vesuvius tephra

Glasses from Somma-Vesuvius Groups 1 and 2 show minimal overlap, with the Group 1 glasses being saturated to slightly SiO_2-undersaturated and plotting at higher CaO (>2.5 wt%) than the mildly silica undersaturated Group 2 glasses. However, there is a high degree of similarity between glasses produced within each chronological phase.

Within Group 1, Verdoline and Pomici di Base glasses, overlap extensively. Pomici di Base is zoned and extends to less evolved (higher CaO) glasses containing microlites, therefore the Pomici di Base can be identified provided that this less evolved component is recorded in the distal tephra population. If distal tephra analyses record only the more evolved Group 1 Somma-Vesuvius composition, then it becomes more difficult to identify the source eruption using major elements alone. In this case, Pomici di Base can be recognized on the basis of its lower absolute incompatible trace element concentrations (e.g. Zr, Nb, Ce).

Tephras from the Group 2 Plinian eruptions of Somma-Vesuvius (Mercato and Avellino) overlap extensively and can be distinguished using major elements only if the low SiO_2 population of Avellino tephra (corresponding also to the most widely dispersed and volumetrically abundant part of the eruption deposits) is present. Trace element discriminators can provide additional confidence (Nb 'vs' Zr, Ce 'vs' Zr) allowing the Group 2 tephras to be separated. In proximal and medial localities where sufficient tephra are present, Avellino may be distinguished from Mercato on the basis that Avellino is porphyritic, while Mercato is aphyric. However these characteristics are less evident in distal localities where only a small number of shards are present and where crystal phases may not be represented.

6. Neapolitan eruptions without a confirmed source

New glass data was also acquired for tephra beds found medially to the Neapoliatan volcanic area, Schiava and Codola, which are thought to have erupted from Somma-Vesuvius but it has not confirmed (Santacroce et al., 2008). These new major and trace element glass data from these units is also compared to that of the three volcanoes in the Neapolitan volcanic area to identify their source volcano.

6.1 Codola

The 30.680 ± 0.780 cal. ka BP (Giaccio et al., 2008; Bronk Ramsey, this issue; Di Vito et al., 2008) Codola eruption is recognized in several medial locations between the Visciano Plateau and the Sorrentina Peninsula (Di Vito et al., 2008). It is clearly from a Campanian source but it is not clear whether it is from Campi Flegrei (Sulpizio et al., 2003) or Somma-Vesuvius (Santacroce et al., 1987, Giaccio et al., 2008, Sulpizio et al., 2010). The Codola tephra has also been reported from a borehole succession drilled at Trecase on the southern slope of Vesuvius (Brocchini et al., 2001), possibly supporting a source at Somma-Vesuvius.

We have analysed the major and trace element composition of the Codola glass, and compared it to the fields defined for Somma-Vesuvius, Campi Flegrei and Ischia (Fig. 5,7). The studied Codola glasses span a narrow range of compositions (57.0-59.7 wt% SiO_2; 3.8-6.3 wt% CaO) and overlap with the Somma-Vesuvius field on major element plots. They also have higher CaO than the products of the other Neapolitan sources (Fig. 5d). This supports a source at Somma-Vesuvius. In particular, the Codola tephra shows significant major element overlap with the Group 1 Somma-Vesuvius products (Verdoline and Pomici di Base). Relative to the other Somma-Vesuvius Group 1 tephras, the composition of the Codola tephra is offset to higher Ta, Nb for a given Zr (Nb/Zr = 0.22 ± 0.02; Ta/Zr = 0.011 ± 0.001; Fig. 7e) and forms a distinct field on plots of REE (e.g. Ce) versus Zr (Fig. 7f). The composition of Codola glasses supports an origin at Somma-Vesuvius and suggests that it represents an earlier group 1 magma, possibly during the growth of the Somma stratocone.

6.2 Schiava

The ~36 ka Schiava Pumice is described in several medial locations on the Appenine mountains bordering the Campanian Plain (Sulpizio et al, 2003; Zanchetta et al., 2004). It has previously been linked to activity at Ischia (Sulpizio et al., 2003). However, the Schiava pumice has been tentatively linked to a ~60m thick layer in a core drilled at Camaldoli della Torre on the southern slopes of Somma–Vesuvius (Di Renzo et al., 2007), if this correlation is correct then it clearly originated from Somma-Vesuvius (Di Vito et al., 2008).

We have analysed the major and trace element composition of Schiava glass, and compared it to the fields defined for Somma-Vesuvius, Campi Flegrei and Ischia (Fig. 5,7). The Schiava tephra is trachytic with a higher SiO_2 content (64.4 ± 0.7 wt%) than the other Neapolitan tephras studied, but does fall within the Somma-Vesuvius field on a MgO-CaO plot (Fig. 5d) and Zr/Sr vs Th (Fig. 6a) consistent with a Somma-Vesuvius source. However, the Schiava glasses are distinct from the other studied Somma-Vesuvius tephras, characterized by higher SiO_2 (Fig. 7a) and also lower K_2O and FeO. In terms of trace elements, Schiava glasses sit on the same trend as Verdoline in Nb-Zr and REE-Zr plots (Fig. 7e,f), but define distinct trends in other elements, with lower Ta/Zr (0.006 ± 0.002) and higher Th/Zr. However, Schiava is significantly different from the studied Campi Flegrei and Ischia glasses, which cover the relevant age range. Therefore, the composition of Schiava glasses supports an origin at Somma-Vesuvius, but may mark an earlier group of activity that is geochemically distinct from the group 1 activity of Codola, Pomici di Base and Verdoline and, as such define a group 0.

7. Conclusions

The central and eastern Mediterranean provides an ideal case study for investigating the diversity of tephra compositions and for defining tools for identifying tephra from different tectonic settings. Variations in ratios of the LILE (e.g. K, Ba Rb) and Y to the HFSE (e.g. Nb, Ta) can be used to distinguish between tephras produced in areas of active subduction, post-subduction and anorogenic (extension-related and intraplate hot spot) settings. The glass composition varies between different sources and eruptions as it reflects source heterogeneity, variable degrees of fractional crystallization, magma mixing, and crustal contamination. These are fundamentally different between different settings therefore allowing the tectonic setting to be identified using the chemical composition. The discrimination diagrams presented (Fig. 4) can be used to narrow down the origin of unknown tephras, which is of particular use for cryptotephra studies that identify ash that has travelled hundreds to thousands of kilometres from source. The detailed glass compositional data allow tephra from the Neapolitan volcanoes, Somma-Vesuvius, Campi Flegrei and Ischia, to be separated using major elements - Na_2O/K_2O-CaO and CaO-MgO (Fig. 5). Applying the criteria to the Codola tephra and Schiava pumice deposits supports previous correlations to Somma-Vesuvius Group 1. However, Schiava appears to represent an earlier eruption that is not exposed in proximal deposits.

Distinguishing between tephra produced during different eruptions from a single volcano is more problematic, and may not be possible without good chronological, stratigraphic controls and/or high-resolution trace element glass data. This is the case for tephra of the large explosive eruptions of Somma-Vesuvius between 4 and 22 ka. Glass compositions of the tephras in the different groups (defined by chronology) overlap extensively on many of the major and trace elements, but can be separated using CaO. There is extensive overlap between glasses within each group making it hard to correlate to individual eruption deposits. However, Pomici di Base is compositionally zoned and so can be distinguished from Verdoline (Group 1), likewise Avellino is compositionally zoned and so can be separated from Mercato (Group 2) provided that full compositional range is present in the distal tephra deposit. With small distal tephra populations, where only glass shards can be safely recovered and in the absence of any other additional information (mineral paragenesis, lithic fragments, morphology and texture of the glass shards), trace element discriminators (Zr, Nb, Ce) and chronostratigraphic constraints become essential to separate similar tephras with confidence.

Acknowledgments:

This work is funded by the NERC RESET Consortium (NE/ E015905/1). This is paper number ROX/00XX. We thank Roberto Sulpizio and an anonymous reviewer, whose comments improved the content and structure of this manuscript. The authors wish to thank all RESET collaborators involved in this work.

References

Albert, P. G., Hardiman, M., Keller, J., Tomlinson, E. L., Smith, V. C., Bourne, A. J., Wulf, S., Zanchetta, G., Sulpizio, R., Muller, U.C., Pross, J., Ottolini, L., Matthews , I.P., Blockley, S.P.E., Menzie, M.A. (In Press). Revisiting the Y-3 tephrostratigraphic marker: a new diagnostic glass geochemistry, age estimate, and details on its climatostratigraphical context. *Quaternary Science Reviews*. doi:10.1016/j.quascirev.2014.04.002

Albert P.G., Tomlinson, E.L., Lane, C.S., Wulf, S., Smith, V.C., Coltelli, M., Keller, J., Castro, D., Manning, C.J., Müller, W., Menzies, M.A. (2013) Late glacial explosive activity on Mount Etna: Implications for proximal–distal tephra correlations and the synchronisation of Mediterranean archives. *J. Volcanol. Geotherm. Res*, 265, 9-26.

Albert, P.G., Tomlinson, E.L. Smith, V.C., Di Roberto, A., Todman, A., Rosi, M., Marani, M., Muller, W., Menzies, M.A. (2012) Marine-continental tephra correlations: Volcanic glass geochemistry from the Marsili Basin. and the Aeolian Islands, Southern Tyrrhenian Sea, Italy. *J. Volcanol. Geotherm. Res*, 229-230, 74-94.

Albert, P.A. (2012) Volcanic glass geochemistry of Italian proximal deposits linked to distal archives in the central Mediterranean region. Ph.D Thesis, Royal Holloway University of London.

Aldanmaz, E., Pearce, J.A., Thirlwall, M.F. and Mitchell, J.G. (2000). Petrogenetic evolution of late Cenozoic, post-collision volcanism in western Anatolia, Turkey. Journal of Volcanology and Geothermal Research, 102, 67-95.

Allen RM, Nolet G, Morgan WJ, Vogfjord K, Nettles M, Ekstrom G, Bergsson BH, Erlendsson P, Foulger GR, Jakobsdottir S. (2002) Plume-driven plumbing and crustal formation in Iceland. *J. Geophys. Res.* 107(B8), 10.1029/2001JB000584

Andronico, D., Cioni, R., 2002. Contrasting styles of Mount Vesuvius activity in the period between the Avellino and Pompeii Plinian eruptions, and some implications for assessment of future hazards. Bull. Volcanol. 64, 372–391.

Andronico, D., Calderoni, G., Cioni, R., Sbrana, A., Sulpizio, R., Santacroce, R., 1995. Geological map of Somma-Vesuvius volcano. Period. Mineral. 64, 77–78.

Arienzo I., Civetta L., Heumann A., Wörner G., Orsi G. - 2009 - Isotopic Evidence for open system processes within the Campanian Ignimbrite magma chamber. Bull. Volcanol., 71: 285–300, doi:10.1007/s00445-008-0223-0.

Arienzo, I., Moretti, R., Civetta, L., Orsi, G. & Papale, P (2010). The feeding system of Agnano–Monte Spina eruption (Campi Flegrei, Italy): Dragging the past into present activity and future scenarios. *Chemical Geology* 270, 135–147.

Arnò, V., Principe, C., Rosi, M., Santacroce, R., Sbrana, A., Sheridan, M.F., 1987. Eruptive history. In: Santacroce, R. (Ed.), Somma–Vesuvius. CNR, Quaderni della Ricerca Scientifica, vol. 8 (114), pp. 53–103.

Auger, E., Gasparini, P., Virieux, J. & Zollo, A (2001). Seismic evidence of an extended magmatic sill under Mt. Vesuvius. *Science* 294, 1510–1512.

Aulinas, M. *et al.* (2007) The 'Pomici di mercato' Plinian eruption of Somma-Vesuvius: magma chamber processes and eruption dynamics. *Bull Volcanol* **70,** 825–840

Ayuso, R.A., De Vivo, B., Rolandi, G., Seal II, R.R., Paone, A., 1998. Geochemical and isotopic (Nd–Pd–Sr–O) variations bearing on the genesis of volcanic rocks from Vesuvius, Italy. J. Volcanol. Geotherm. Res. 82, 53–78.

Barberi, F., Leoni L. (1980), Metamorphic carbonate ejecta from Vesuvius Plinian eruptions: Evidence of the occurrence of shallow magma chambers, Bull. Volcanol., 43, 108-120.

Barton RNE, Lane C, Albert PG, White D, Collcutt SN, Bouzouggar A, Ditchfield P, Farr L, Oh A, Ottolini L, Smith VC, Van Peer P and Kindermann, K (this volume) The role of cryptotephra in refining the chronology of Late Pleistocene human evolution and cultural change in North Africa

Belkin, H. E., De Vivo B. (1993), Fluid inclusion studies of ejected nodules from Plinian eruptions of Mt. Somma-Vesuvius, J. Volcanol. Geotherm. Res., 58, 98-100

Benson L Liddicoat J Smoot J Sarna-Wojcicki A Negrini R and Lund S (2003) Age of the Mono Lake excursion and associated tephra. *Quat. Sci. Rev*. 22 pp. 135–140

Bertagnini, A., Landi, P., Rosi, M., Vigliargio, A., 1998. The Pomici di Base Plinian eruption of Somma–Vesuvius. J. Volcanol. Geotherm. Res. 83, 219–239.

Bird P (1979). Continental delamination and the Colorado Plateau. *Journal of Geophysical Research*, 84, 7561–7571.

Brocchini D, Principe C, Castradori D, Laurenzi MA, Gorla L (2001) Quaternary evolution of the southern sector of the Campanian Plain and early Somma–Vesuvius activity: insights from the Trecase1 well. *Mineralogy and Petrology*, 73, 67–91

Bronk Ramsey, C., Albert, P., Blockley, S.P.E., Hardimam, M.. Housley, R.A., Lane, C.S., Lee, S., Matthews, I.P., Smith, V.C., Lowe, J. (this issue) The Chronology of the RESET Tephra Lattice. Quaternary Science Reviews.

Brown RJ, Orsi G, de Vita S (2008). New insights into Late Pleistocene explosive volcanic activity and caldera formation on Ischia (southern Italy). Bulletin of Volcanology 70:583–603.

Bruno P, de Alteriis G, Florio G (2002) The western undersea section of the Ischia volcanic complex (Italy, Tyrrhenian Sea) inferred by marine geophysical data. Geophys Res Let 29: Art. No. 1343.

Buchner G, Italiano A, Vita-Finzi C (1996) Recent upift of Ischia, Southern Italy. In: Jones, W. J., Jones, A. P., and Neuberg, J. (Eds) Volcano instability on the Earth and other planets, Geol Soc Spec Pub 110: 249–252.

Capaldi, G., Gillot, P.Y., Munno, R., Orsi, G., Rolandi, G., 1985. The Sarno formation: the major plinian eruption of the Somma–Vesuvius. IAVCEI 1985 Scientific Assembly, Giardini Naxos (Italy), September 1–21, 1985. abstracts volume.

Capuano P., Russo G., Civetta L., Orsi G., D'Antonio M., Moretti R. - 2013 - The Campi Flegrei caldera structure imaged by 3-D inversion of gravity data. Geochem. Geophys. Geosyst., 14: 4681-4697, doi:10.1002/ggge.20276.

Cioni, R., 2000. Volatile content and degassing processes in the AD 79 magma chamber at Vesuvius (Italy). Contrib. Mineral. Petrol. 140, 40–54.

Cioni, R., Bertagnini, A., Santacroce, R. & Andronico, D. (2008) Explosive activity and eruption scenarios at Somma-Vesuvius (Italy): Towards a new classification scheme. *Journal of Volcanology and Geothermal Research* 178, 331–346.

Cioni, R., Sulpizio, R., Garruccio, N., 2003. Variability of the eruption dynamics during a subplinian event: the Greenish Pumice eruption of Somma–Vesuvius (Italy). *J. Volcanol. Geotherm. Res.* 124, 89–114.

Civetta L, Gallo G, Orsi G (1991) Sr- and Nd-isotope and trace element constraints on the chemical evolution of Ischia (Italy) in the last 55 ka. J Volcanol Geotherm Res 46:213–230

Civetta, L., D'Antonio, M., de Lorenzo, S., Di Renzo, V. & Gasparini, P. (2004). Thermal and geochemical constraints on the 'deep' structure of Mt. Vesuvius. Journal of Volcanology and Geothermal Research 133, 1-12.

Coltelli, M., Del Carlo, P., Vezzoli, L., 2000. Stratigraphic constraints for explosive activity in the past 100 ka at Etna Volcano, Italy. International Journal of Earth Sciences 89, 665–667.

Cross JK, Tomlinson EL, Giordano G, Smith VC, De Benedetti AA, J. Roberge, C. Manning, S. Wulf, M.A. Menzies (2014) High level triggers for explosive mafic volcanism: Albano Maar, Italy. *Lithos*, 190-191, 137-153.

D'Antonio M., Tonarini S., Arienzo I., Civetta L., and Di Renzo V. (2007) Components and processes in the magma genesis of the Phlegraean Volcanic District, Southern Italy. In Cenozoic volcanism in the Mediterranean area, Vol. 418 (ed. L. Becca- luva, G. Bianchini, and M. wilson), pp. 203–220. Geological Society of America Special Publication.

Davies SM Abbott PM Pearce NJG Wastegård S and Blockley SEP (2012). Integrating the INTIMATE records using tephrochronology: rising to the challenge. *Quaternary Science Reviews 36,* 11-27.

Davies, JH and Von Blanckenburg F. (1995). Slab breakoff: a model of lithospheric detachment and its test in the magmatism and deformation of collisional orogens. *Earth and Planetary Science Letters*, 129, 85–102

Doglioni, C (1991) A proposal of kinematic modelling for W-dipping subductions—possible applications to the Tyrrhenian – Apennines system. Terra Nova, 3, 423–434.

De Vita, S., Orsi, G., Civetta, L., Carandente, A., D'Antonio, M., Deino, A., et al. (1999). The Agnano–Monte Spina eruption (4100 years BP) in the restless Campi Flegrei caldera (Italy). *Journal of Volcanology and Geothermal Research*, *91*(2), 269–301.

De Vivo B, Rolandi G, Gans PB, Calvert A, Bohrson WA, Spera FJ Belkin HE (2001) New constraints on the pyroclastic eruptive history of the Campanian volcanic Plain (Italy). *Miner Petrol* 73: 47–65

Deino AL, Orsi G, de Vita S Piochi M (2004) The age of the Neapolitan Yellow Tuff caldera-forming eruption (Campi Flegrei caldera Italy) assessed by Ar-40/Ar-39 dating method*. J Volcanol Geoth Res* 133: 157–170

Di Renzo V., Arienzo I., Civetta L., D’Antonio M., Tonarini S., Di Vito M. A. and Orsi G. (2011) The magmatic feeding system of the Campi Flegrei caldera: Architecture and temporal evolution. Chem. Geol. 281(3–4), 227–241.

Di Renzo V., Di Vito M. A., Arienzo I., Carandente A., Civetta L., D’Antonio M., Giordano F., Orsi G. and Tonarini S. (2007) Magmatic history of Somma-Vesuvius on the basis of new geochemical and isotopic data from a deep borehole (Camaldoli della Torre). J. Petrol. 48(4), 753–784.

Di Vito M. A., Isaia R., Orsi G., Southon J., de Vita S., D’Antonio M., Pappalardo L. and Piochi M. (1999) Volcanism and deformation since 12,000 years at the Campi Flegrei caldera (Italy). J. Volcan. Geoth. Res. 91(2–4), 221–246.

Di Vito M. A., Sulpizio R., Zanchetta G., and D’Orazio M. (2008) The late Pleistocene pyroclastic deposits of the Campanian Plain: new insights into the late Pleistocene pyroclastic deposits of the Campanian Plain: new insights into the explosive activity of Neapolitan volcanoes. *J. Volcan. Geoth. Res.*, 177(1), 19-48.

Druitt, T. H., L. Edwards, R. M. Mellors, D. M. Pyle, R. S. J. Sparks, M. Lanphere, M. Davies, and B. Barriero (1999), Santorini Volcano, vol. 19, Chapter 3, Geol. Soc. Lond. Memoir.

Dugmore AJ, Larsen G, Newton AJ (1995) Seven tephra isochrones in Scotland. The Holocene 5: 257–266

Ellam RM and Hawkesworth CJ (1988) Elemental and isotope variations in subduction related basalts: Evidence for a three component model. Contrib. Mineral. Petrol., 98, 72–80

Fabbro, G. N.; Druitt, T. H.; Scaillet, S. (2013) Evolution of the crustal magma plumbing system during the build-up to the 22-ka caldera-forming eruption of Santorini (Greece). Bulletin of Volcanology , 75 (12), 767.

Freda, C., Gaeta, M., Karner, D.B., Marra, F., Renne, P.R., Taddeucci, J., Scarlato, P., Christensen, J.N., Dallai, L., 2006. Eruptive history and petrologic evolution of the Albano multiple maar (Alban Hills, Central Italy). Bulletin of Volcanology 68, 567–591.

Frazzetta G, La Volpe L & Sheridan MF (1983) Evolution of the Fossa cone, Vulcano. Journal of Volcanology and Geothermal Research 17: 329-360

Froese, DG, Lowe DJ, Knott, J and Slate, JL (2008) Preface – global tephra studies. Quaternary International, 178, 1–3

Frost BR, Arculus RJ, Barnes CG, Collins WJ, Ellis DJ, Frost CD (2001) A geochemical classification of granitic rocks. *Journal of Petrology,* 42,2033-2048.

Gaeta, M., Freda, C., Marra, F., Di Rocco, T., Gozzi, F., Arienzo, I., Giaccio, B., Scarlato, P., 2011. Petrology of the most recent ultrapotassic magmas from the Roman Province (Central Italy). Lithos 127 (1–2), 298–308.

Gertisser, R., Self, S., Gaspar, J. L., Kelley, S. P., Pimentel, A., Eikenberg, J., et al. (2010). Ignimbrite stratigraphy and chronology on Terceira Island, Azores. In *Geological Society of America Special Paper* (Vol. 464, pp. 133–154)

Giaccio, B., Isaia, R., Fedele, F.G., Di Canzio, E., Hoffecker, J., Ronchitelli, A., Sinitsyn, A., Anikovich, M., Lisitsyn, S.N., (2008). The Campanian Ignimbrite and Codola tephra layers: two temporal/stratigraphic markers for the Early Upper Palaeloithic in southern Italy and eastern Europe. J*. Volcanol. Geotherm. Res*. 107, 208-226.

Gill JB (1981) Orogenic Andesites and Plate Tectonics, Springer, Berlin, p. 390

Hawksworth CJ, Gallagher K, Hergt JM, McDermott F. (1994) Destructive plate margin magmatism: Geochemistry and melt generation. Lithos 33(1-3), 69-188.

Hawkesworth, C., Turner, S., Gallagher, K., Hunter, A., Bradshaw, T. & Rogers, N. (1995) Calc-alkaline magmatism, lithospheric thinning and extension in the Basin and Range. Journal of Geophysical Research, 100, 10271-20286.

Houseman, G. A., McKenzie DP and Molnar P J (1981). Convective instability of a thickened boundary layer and its relevance for the thermal evolution of continental convergent belts. *Journal of Geophysical Research*, 86, 6115–6132.

Johnson, R.W., Mackenzie, D.E. & Smith, I.E.M. 1978. Delayed partial melting of subduction-modified mantle in papua new guinea. Tectonophysics, 46, 197-216.

Joron JL, Metrich N, Rosi M, Santacroce R, Sbrana A. (1987) Chemistry and petrography. In: Santacroce, R. Ed., Somma Vesuvius. CNR Quad. Ric. Sci. 114, 105–174.

Judenherc S, Zollo A (2004) The Bay of Naples (southern Italy): Constraints on the volcanic structures inferred from a dense seismic survey. J. Geophysical Res. Solid Earth 109(B10), B10312

Karkanas, P., White, D., Lane, C.S., Cullen, V.L., Stringer, C., Davies, S.W.G., Smith, V.C., Tomlinson, E.L., Ntinou, M., Tsartsidou, G. and Kyparissi-Apostolika, N (this issue) Tephra chronostratigraphy and climatic events between the MIS6/5 transition and the beginning of MIS3 in Theopetra Cave, central Greece. Quaternary Science Reviews.

Keller, J., 2002. Lipari's fiery past: dating the Medieval pumice eruption of Monte Pelato, Internat. Conference UNESCO-Reg Siciliana, Lipari, September 29–October 2.

Kieffer, G., 1979. L'activité de l'Etna pendant les dernières 20000 ans. Comptes Rendus de l' Academie des Sciences Paris 288D, 1023–1026.

Landi P, Bertagnini A, Rosi M (1999) Chemical zoning and crystallization mechanisms in the magma chamber of the Pomici di Base plinian eruption of Somma-Vesuvius (Italy). Contrib. Miner. Petrol. 135, 179-197.

Lane, C.S., Andrič, M., Cullen, V.L., Blockley, S.P.E. 2011. The occurrence of distal Icelandic and Italian tephra in the Lateglacial of Lake Bled, Slovenia. Quaternary Science Reviews, 30, 1013-1018.

Lane, C.S., Chorn, B.T., Johnson, T.C. (2013a). Ash from the Toba super-eruption in Lake Malawi shows no volcanic winter in East Africa at 75 ka. Proceedings of the National Academy of Science, 110, 20, 8025–8029.

Lane, CS, Brauer A, Blockley SPE and Dulski P. (2013b) Volcanic ash reveals time-transgressive abrupt climate change during the Younger Dryas. Geology, 41(12), 1251-1254.

Le Maitre R. W. (1989) A Classification of Igneous Rocks and Glossary of terms: Recommendations of the International Union of Geological Sciences Subcommission on the Systematics of Igneous Rocks. Blackwell Scientific Publications, Oxford, UK.

Lowe J. Barton N. Blockley S. Ramsey C.B. Cullen V.L. Davies W. Gamble C. Grant K. Hardiman M. Housley R. Lane C.S. Lee S. Lewis M. MacLeod A. Menzies M. Muller W. Pollard M. Price C. Roberts A.P. Rohling E.J. Satow C. Smith V.C. Stringer C.B. Tomlinson E.L. and White D. (2012). Volcanic ash layers illuminate the resilience of Neanderthals and early modern humans to natural hazards. *Proceedings of the National Academy of Sciences,* 109 13532–13537.

Lowe JJ, Rasmussen, SO, Björck, S, Hoek, WZ, Steffensen JP, Walker, MJC and Yu, Z (2008a) INTIMATE group Synchronisation of palaeoenvironmental events in the North Atlantic region during the Last Termination: a revised protocol recommended by the INTIMATE group. *Quaternary Science Reviews*, 27, 6–17.

Lowe, J, Shane, PAR, Alloway BV and Newnham, RM (2008b) Fingerprints and age models for widespread New Zealand tephra marker beds erupted since 30,000 years ago: a framework for NZ-INTIMATE. *Quaternary Science Reviews*, 27, 95–126.

Mangiacapra A, Moretti R, Rutherford M, Civetta L, Orsi G and Papale P (2008)The deep magmatic system of the Campi Flegrei caldera (Italy). *Geophysical Research Letters* 35(21), L21304.

Manning SW, Ramsey CB, Kutschera W, Higham T, Kromer B, Steier P, Wild EM (2006) Chronology for the Aegean Late Bronze Age 1700-1400 BC. Science, 312, 565-569.

Marianelli P, Sbrana A, Proto M. (2006) Magma chamber of the Campi Flegrei supervolcano at the time of eruption of the Campanian Ignimbrite. Geology 34(11), 937- 940

Marianelli, P., Sbrana, A., Metrich, N. & Cecchetti, A (2005). The deep feeding system of Vesuvius involved in recent violent strombolian eruptions. *Geophys. Res. Lett.* 32

Morche, W., 1988. Tephrochronologie der Aolischen Inseln. Unpublished Thesis, Albert-Ludwigs-Universitat Freiburg, Germany.

Moretti R, Arienzo I, Orsi G, Civetta L, D'Antonio M (2013) The Deep Plumbing System of Ischia: a Physico-chemical Window on the Fluid-saturated and CO_2-sustained Neapolitan Volcanism (Southern Italy). Journal of Petrology, 54 (5), 954-981.

Nunziata C (2010*)* Low shear-velocity zone in the Neapolitan-area crust between the Campi Flegrei and Vesuvio volcanic areas. Terra Nova, 22(3) 208-217.

Orsi G., de Vita S., Di Vito M., Isaia R., Nave R., Heiken G. - 2003 - Facing volcanic and related hazards in the Neapolitan area. In (Heiken G., Fakundiny R., Sutter J., Edits) "Earth Sciences in the Cities: A Reader", Am. Geophys. Un., Sp. Publ. Series, 56: 121-170.

Orsi G, Gallo G, Zanchi A (1991) Simple-shearing block resurgence in caldera depressions. A model from Pantelleria and Ischia. J Volcanol Geotherm Res 47: 1–11

Orsi G, Patella D, Piochi M and Tramacere A (1999) Magnetic modeling of the Phlegraean Volcanic District with extension to the Ponza archipelago, Italy. Journal of Volcanology and Geothermal Research, 91(2-4) 345-360.

Orsi G., de Vita S. and Di Vito M. A. (1996) The restless, resurgent Campi Flegrei nested caldera (Italy): Constraints on its evolution and configuration. J. Volcan. Geoth. Res. 74(3–4), 179–214.

Orsi G., Di Vito M. A. and Isaia R. (2004) Volcanic hazard assessment at the restless Campi Flegrei caldera. B. Volcanol. 66(6), 514–530.

Pabst S., Worner G., Civetta L. and Tesoro R. (2008) Magma chamber evolution prior to the Campanian Ignimbrite and Neapolitan Yellow Tuff eruptions (Campi Flegrei, Italy). B. Volcanol. 70(8), 961–976.

Paoletti, V., D'Antonio, M. & Rapolla, A. (2013) The structural setting of the Ischia Island (Phlegrean Volcanic District, Southern Italy): Inferences from geophysics and geochemistry. *Journal of Volcanology and Geothermal Research* 249, 155–173.

Paone, A., 2005. Evidence of crustal contamination, sediment, and fluid components in the campanian volcanic rocks. J. Volcanol. Geotherm. Res. 138, 1–26.

Pappalardo L., Civetta L., D'Antonio M., Deino A., Di Vito M. A., Orsi G., Carandente A., de Vita S., Isaia R. and Piochi M. (1999) Chemical and Sr-isotopical evolution of the Phlegraean magmatic system before the Campanian Ignimbrite and the Neapolitan Yellow Tuff eruptions. J. Volcan. Geoth. Res. 91(2– 4), 141–166.

Pappalardo L., Piochi M., D'Antonio M., Civetta L. and Petrini R. (2002) Evidence for multi-stage magmatic evolution during the past 60 kyr at Campi Flegrei (Italy) deduced from Sr, Nd and Pb isotope data. J. Petrol. 43(8), 1415–1434.

Platevoulet B, Scaillet S, Guillou H, Blamart D, Nomade S, Massault M, Poisson A, Elitok Ö, Özgür N, Yağmurlu F, Yılmaz K (2008) Pleistocene eruptive chronology of the Gölcük volcano, Isparta Angle, Turkey, Quaternaire, 19, 147-156

Pearce JA and Peate DW (1995) Tectonic implications of the composition of volcanic arc magmas. Annual Review of Earth and Planetary Sciences 23, 51-285.

Pearce JA, Harris NBW and Tindal AG (1984) Trace Element Discrimination Diagrams for the Tectonic Interpretation of Granitic Rocks. *J. Petrology,* 25, 956-983.

Peccerillo A (2005) Plio-Quaternary volcanism in Italy. Petrology, Geochemistry, Geodynamics. Springer, Heidelberg, 365 pp

Peccerillo A and Manetti (1985). The potassium alkaline volcanism of central-southern Italy: a review of the data relevant to petrogenesis and geodynamic significance. Trans. Geol. Soc. S. Africa, 88, 379-394.

Peccerillo A, Taylor SR (1976) Geochemistry of Eocene calc-alkaline volcanic rocks of the Kastamonu area, northern Turkey. *Contrib Mineral Petrol* 58:63-81

Petrone, C.M., Braschi, E., Francalanci, L., 2009. Understanding the collapse–eruption link at Stromboli, Italy: a microanalytical study on the products of the recent Secche di Lazzaro phreatomagmatic activity. Journal of Volcanology and Geother- mal Research 188 (4), 315–332.

Piochi M, Civetta L, Orsi G (1999) Mingling in the magmatic system of Ischia (Italy) in the past 5 ka. Min Pet 66: 227–258

Platt JP and Vissers RLM (1989). Extensional collapse of thickened continental lithosphere: a working hypothesis for the Alboran Sea and the Gibraltar Arc. *Geology*, 17, 540–543.

Poli S, Chiesa S, Gillot P-Y, Gregnanin A, Guichard F (1987) Chemistry versus time in the volcanic complex of Ischia (Gulf of Naples, Italy): evidence of successive magmatic cycles. Contrib Min Pet 95:322–335

Pyne-O'Donnell SDF, Hughes PDM, Froese DG, Jensen BJL' Kuehn SC, Mallon G, Amesbury MJ, Charman DJ, Daley TJ, Loader NJ, Mauquoy D, Street-Perrott FA and Woodman-Ralph J (2014) High-precision ultra-distal Holocene tephrochronology in North America. Quaternary Science Reviews, 52, 6-11.

Rapolla A, Fedi M and Fiume MG (1989) Crustal structure of the Ischia-Phlegrean geothermal fields, near Naples, Italy, from gravity and aeromagnetic data. Geophysical Journal Oxford 97(3), 409-419.

Reimer PJ, Bard E, Bayliss A, Beck JW, Blackwell PG., Bronk Ramsey C, Buck CE, Cheng H, Edwards RL, Friedrich M, Grootes PM, Guiderson TP, Hajdas I, Hatte C, Heaton TJ, Hoffman DL, Hogg AG, Hughen KA, Kaiser KF, Kromer B, Manning SW, Niu M, Reimer RW, Richards DA, Scott EM, Southon JR, Staff RA, Turney CSM and van der Plicht J (2013) IntCal13 and Marine13 Radiocarbon Age Calibration Curves 0–50,000 Years cal BP. *Radiocarbon* 55(4), 1869-1887.

Rolandi G., Bellucci F., Heizler M. T., Belkin H. E. and De Vivo B. (2003) Tectonic controls on the genesis of ignimbrites from the Campanian Volcanic Zone, southern Italy. Miner. Petrol. 79, 3–31.

Santacroce, R. (Ed.), 1987. Somma-Vesuvius. Quaderni della Ricerca Scientifica, vol. 8, 114. CNR, pp. 1–251.

Santacroce, R., Cioni, R., Marianelli, P., Sbrana, A., Sulpizio, R., Zanchetta, G., Donahue, D. J., Joron, J.L., (2008) Age and whole-rock-glass compositions of proximal pyroclastics from the major explosive eruptions of Somma-

Vesuvius: a review as a tool for distal tephrostratigraphy. J. Volcanol. Geotherm. Res.

Santacroce R., Cristofolini R., La Volpe L., Orsi G., Rosi M. - 2003 - Italian Active Volcanoes. Episodes, 26, 3: 227-234.

Sarimathkaya, M. A., Zreda, M., & Ciner, A. (2009). Glaciations and paleoclimate of Mount Erciyes, central Turkey, since the Last Glacial Maximum, inferred from ^{36}Cl cosmogenic dating and glacier modeling. *Quaternary Science Reviews*, *28*(23-24), 2326–2341. doi:10.1016/j.quascirev.2009.04.015

Sartori R (2003) The Tyrrhenian back-arc basin and subduction of the Ionian lithosphere. Episodes 26(3) 127-221.

Scaillet, B., Pichavant, M. & Cioni, R (2008). Upward migration of Vesuvius magma chamber over the past 20,000 years. *Nature* 455, 216–219

Scandone P. (1979) Origin of the Tyrrhenian Sea and Calabrian Arc. Boll. Soc. Geol. It., 98, 27-34

Schmitt, A.K., Danisik, M., Evans, N.J., Siebel,W., Kiemele,E., Aydin,F., Harvey,J., (2011). Acigöl rhyolite field, Central Anatolia (part 1): high-resolution dating of eruption episodes and zircon growth rates. *Contributions to Mineralogy and Petrology*, v.162, Issue 6, pp 1215-1231.

Selva J., Orsi G., Di Vito M., Marzocchi W., Sandri L. - 2012 - *Probability hazard map for future vent opening at the Campi Flegrei caldera, Italy*. Bull. Volcanol., 74: 497-510, doi:10.1007/s00445-011-0528-2.

Serri, G. (1997), Neogene-Quaternary magmatic activity and its geodynamic implications in the central Mediterranean region, Ann. Geofisica, 3, 681–703.

Serri, G., Innocenti, F. anf Manetti, P. (1993) Geochemical and petrological evidence of the subduction of delaminated Adriatic continental lithosphere in the genesis of the Neogene – Quaternary magmatism of central Italy. Tectonophysics, 223, 117–147.

Sevink, J., van Bergen, M. J., van der Plicht, J., Feiken, H., Anastasia, C., & Huizinga, A. (2011). Robust date for the Bronze Age Avellino eruption (Somma-Vesuvius): 3945 ± 10 calBP (1995 ± 10 calBC). Quaternary Science Reviews, 30, 1035-1046. doi:10.1016/j.quascirev.2011.02.001

Seyitoglu, G. & Scott, B.C. (1996) The cause of N_S extensional tectonics in Western Turkey: tectonic escape vs. back-arc spreading vs orogenic collapse. Journal of Geodynamics, 22, 145-153.

Smith, V. C., Pearce, N. J. G., Matthews, N. E., Westgate, J. A., Petraglia, M. D., Haslam, M., Lane, C.S., Korisettar, R., Pal, J.N. (2011a). Geochemical fingerprinting of the widespread Toba tephra using biotite compositions. *Quaternary International*, 246(1-2), 97–104. doi:10.1016/j.quaint.2011.05.012

Smith V. C., Isaia R. and Pearce N. J. (2011b) Tephrostratigraphy and glass compositions of post-15 kyr Campi Flegrei eruptions: implications for eruption history and chronostratigraphic markers. *Quaternary Science Reviews* 30(25–26), 638–3660.

Smith, V. C., Shane, P., & Nairn, I. A. (2005). Trends in rhyolite geochemistry, mineralogy, and magma storage during the last 50 kyr at Okataina and Taupo volcanic centres, Taupo Volcanic Zone, New Zealand. *Journal of Volcanology and Geothermal Research*, *148*(3-4), 372–406.

Sulpizio, R. *et al.* (2010) The Pomici di Avellino eruption of Somma-Vesuvius

(3.9 ka bp). Part I: stratigraphy, compositional variability and eruptive dynamics. *Bull Volcanol* **72,** 539–558.

Sulpizio, R., Zanchetta, G., Paterne, M., Siani, G., 2003. A review of tephrostratigraphy in central and southern Italy during the last 65 ka. Il Quaternario 16, 91–108.

Sulpizio, R, Zanchetta, G, D'Orazio, M, Vogel, H and Wagner, B. (2010) Tephrostratigraphy and tephrochronology of lakes Ohrid and Prespa, Balkans. Biogeosciences, 7, 3273-3288.

Sun S.-S. and McDonough W. F. (1989) Chemical and isotopic systematics of oceanic basalts: implications for mantle compo- sition and processes. In Magmatism in Ocean Basins, Vol. 42 (ed. A. D. Saunders, Norry, M.J.), pp. 313–345. Geological Society of London Special Publication.

Sevink, J, van Bergen, MJ, van der Plicht, J, Feiken, H, Anastasia, C and Huizinga A (2011) Robust date for the Bronze Age Avellino eruption (Somma-Vesuvius): 3945 ± 10 calBP (1995 ± 10 calBC). Quaternary Science Reviews, 30, 1035-1046

Tatsumi Y (1086) Formation of the volcanic front in subduction zones. Geophysical Research Letters 13(6) 717-720.

Todman, A (2011) Temporal and spatial variations in the geochemistry of recent (<2ka) volcanic rocks from Vulcano, Aeolian Islands, Italy. M.Sc thesis, Royal Holloway University of London.

Tomlinson EL, H.S. Kinvig, V.C. Smith, J.D. Blundy, J. Gotsmann, W. Mueller, and M.A. Menzies (2012a). The Upper and Lower Nisyros Pumices: revisions to the Mediterranean tephrostratigraphic record using glass geochemistry. *Journal of Volcanology and Geothermal Research*, 243-244, 69-80.

Tomlinson EL, I. Arienzo, S, Wulf, V.C. Smith, A. Carandente, L. Civetta, M. Hardiman, C.S. Lane, G. Orsi, M. Rosi, M.T. Thirlwall, W. Muller and M.A. Menzies (2012b). Geochemistry of the Campi Flegrei (Italy) proximal sources for major Mediterranean tephras (C-1, C-2, Y-3 and Y-5). *Geochimica et Cosmochimica Acta* 93, 102-128.

Tomlinson EL, P.G. Albert, S. Wulf, R.J. Brown, V.C. Smith, J. Keller, G. Orsi, A.J. Bourne, M.A. Menzies. Age and geochemistry of tephra layers from Ischia, Italy: constraints from proximal-distal correlations with Lago Grande di Monticchio. Accepted, *Journal of Volcanology and Geothermal Research*.

Tomlinson EL, T. Thordarson, C.S. Lane, C.J. Manning, V.C. Smith, W. Mueller, and M.A. Menzies (2012c). Petrogenesis of the Solheimar Ignimbrite (Katla, Iceland): implications for tephrostratigraphy. *Geochimica et Cosmochimica Acta*, 86, 318-337.

Tomlinson EL, T. Thordarson, W. Mueller , M. Thirlwall, M.A. Menzies (2010). Microanalysis of tephra by LA-ICP-MS - Strategies, advantages and limitations assessed using the Thorsmork ignimbrite (Southern Iceland). *Chemical Geology* 279, 73-89.

Tonarini S., Leeman W. P., Civetta L., D'Antonio M., Ferrara G. and Necco A. (2004) B/Nb and systematics in the Phlegrean Volcanic District (PVD). J. Volcan. Geoth. Res. 113, 123–139.

Turner SP, Platt JP, George RMM, Kelley SP, Pearson DG and Nowell GM (1999). Magmatism associated with orogenic collapse of the Betic – Alboran Domain, SE Spain. Journal of Petrology, 40, 1011–1036.

Turney CSM, Blockley SPE, Lowe JJ, Wulf S, Branch NP, Mastrolorenzo G, Swindle G, Nathan R, Pollard AM (2008) Geochemical characterization of

Quaternary tephras from the Campanian Province, Italy, Quaternary International, 178, 288-30.

Turney CSM, Lowe JJ, Davies SM, Hall VA, Lowe DA, Wastegård S, Hoek WZ, Alloway BV (2004) Tephrochronology of Last Termination sequences in Europe: a protocol for improved analytical precision and robust correlation procedures (a joint SCOTAV–INTIMATE proposal). Journal of Quaternary Science, 19, 111–120.

Vazquez JA and Libzbarski MI (2012) High-resolution tephrochronology of the Wilson Creek Formation (Mono Lake California) and Laschamp event using ^{238}U-^{230}Th SIMS dating of accessory mineral rims. *Earth and Planetary Science Letters* 357-358 54-67.

Vezzoli L (Ed) (1988) Island of Ischia. Quaderni de La Ricerca Scientifica, Consiglio Nazionale delle Ricerca, Rome 114 pp.133

Watts, W.A., Allen, J.R.M., Huntley, B. (1996) Vegetation history and palaeoclimate of the last glacial period at Lago Grande di Monticchio, southern Italy. Quaternary Science Reviews 15, 133–153

Wilson M and Bianchini G (1999) Tertiary–Quaternary magmatism within the Mediterranean and surrounding regions. In: Durand, Jolivet, Horvath and Seranne (eds) The Mediterranean Basins: Tertiary Extension within the Alpine Orogen. Geological Society, London, Special Publications 156, 141 – 168.

Wulf, S., Kraml, M., Brauer, A., Keller, J., Negendank, J.F.W., (2004). Tephrochronology of the 100 ka lacustrine sediment record of Lago Grande di Monticchio (southern Italy). Quaternary International, 122, 7–30.

Wutke K, Wulf S, Tomlinson EL, Hardiman M, Dulski P, Luterbacher J and Brauer A. Large eruptions of Campanian volcanoes at 38-40 ka BP and their environmental impacts - a case study from Lago Grande di Monticchio, Southern Italy. Quaternary Science Reviews, this volume.

Zanchetta, G., Sulpizio, R., Di Vito, M.A., 2004. The role of volcanic activity and climate in alluvial fan growth at volcanic areas: an example from southern Campania (Italy). Sediment. Geol. 168, 249–260.

Zanchetta, G, Sulpizio, R, Roberts, N, Cioni, R, Eastwood, WJ, Siani, G, Caron, B, Paterne, M and Santacroce, R (2011) Tephrostratigraphy, chronology and climatic events of the Mediterranean basin during the Holocene: An overview. The Holocene 21, 33-55.

Zanella, E., De Astis, G., Lanza, R., (2001). Palaeomagnetism of welded, pyroclastic-fall scoriae at Vulcano, Aeolian Archipelago. Journal of Volcanology and Geothermal Research 107 (1–3), 71–86.

Zollo A, Maercklin N, Vassallo M, Dello Iacono D, Virieux J and Gasparini P. (2008) Seismic reflections reveal a massive melt layer feeding Campi Flegrei caldera. Geophysical Research Letters 35(12), L12306.

Zollo, A. *et al (2008)* Seismic reflections reveal a massive melt layer feeding Campi Flegrei caldera. *Geophys. Res. Lett.* 35, L12306.

Tables

Table 1: Summary of information on the eruptions analysed in this study.
Footnote: Ig. = Ignimbrite. Radiocarbon ages are recalibrated from the original publication by Bronk Ramsey et al., this volume ($), and using IntCal13 (Reimer et al., 2013) in this study (*),95% probability range quoted, Year 0 is 1950 AD. Please see references for uncalibrated radiocarbon determinations.

Table 2: Proximal Somma-Vesuvius products. Age references 1 – Sevink et al., 2011; 2 – Zanchetta et al., 2011; 3 - Siani et al., 2004; 4 - Di Vito et al., 2008; 5 – Giaccio et al., 2008. Radiocarbon ages are recalibrated from the original publication by Bronk Ramsey et al., this volume ($), and using IntCal13 (Reimer et al., 2013) in this study (*)., 95% probability range quoted, Year 0 is 1950 AD. Please see references for uncalibrated radiocarbon determinations. Samples from *Di Vito et al., 2008; [$]Cioni et al., 2003; [§]Bertagnini et al., 1998. Mineral abbreviations: san – sanidine, cpx – clinopyroxene, plag – plagioclase, amp – amphibole, bt – biotite.

Table 3: Summary of the overlaps between Campi Flegrei, Ischia and Somma-Vesuvius tephra and the most useful plots for discriminating between these sources.

Table 4: Representative major (wt%) and trace (ppm) element compositions of Somma-Vesuvius glasses, plus glasses from the Codola and Schiava eruptions. Major element totals are normalised to 100 wt.%, the pre-normalised total is also

given. The full dataset is given as online supplementary data.

Figures

Figure 1: Map showing the locations of studied volcanoes in active subduction (red), post subduction back arc spreading (green), post subduction collision (blue) and in anorogenic setttings (black). Red lines indicate the major tectonic structures. Key to volcanos: A – Acigöl, CA - Colli Albani, CF - Campi Flegrei, E – Etna, Er – Erciyes, G – Gölcük, I – Ischia, K – Katla, Li – Lipari, N – Nisyros, P – Pantelleria, S – Santorini, Sa – Salina, St – Stromboli, SV - Somma Vesuvius, T – Tinjafallajökull, Te – Terceira, V – Vulcano.

Figure 2: (a) Glass data normalized to whole-rock data for porphoritic samples from Nisyros (Tomlinson et al., 2012a); (b) microlites in Somma-Vesuvius Pomici di Base sample SM21; (c) plot of glass 'vs' bulk major element composition for microlite-rich and and microlite-poor samples; (d) plot of glass 'vs' bulk trace element composition for microlite-rich (SM21) and microlite-poor (SM28) samples; (e) variation in relative standard deviation with concentration for replicate analyses of major elements in MPI-DING glass standards; (f) variation in relative standard deviation with concentration for replicate analyses of trace elements in MPI-DING glass standards.

Figure 3: (a-e) Major element bivariate plots showing normalised compositions of volcanic glass produced during major <100 ka European explosive eruptions. Errors are 2 s.d. calculated using replicate analyses of MPI-DING StHs6/80 glass.

(f) Primitive mantle normalised trace element compositions of volcanic glass produced during major <100 ka European explosive eruptions. The fields for each tectonic setting enclose the average composition of tephra produced during each eruption (see table 1). Primitive mantle values are from Sun and McDonough (1989).

Figure 4: Tectonic setting discrimination diagrams for: Subduction-related versus anorogenic settings (a) Nb/Rb ‘vs’ Th/Rb; (b) Ta/Rb ‘vs’ U/Rb. Active- and post-subduction: (c) K_2O ‘vs’ SiO_2 dashed line is the boundary between high-K alkaline and the shoshonite-latite field for subduction settings (Peccerillo and Taylor 1976); (d) FeO/(FeO+MgO) ‘vs’ SiO_2, dashed line divides the fields of ferroan and magnesian granites (Frost et al, 2001). Anorogenic, active-subduction and post-subduction: (e) Rb ‘vs’ Y+Nb, grey line shows the fields for whole-rock granitic samples Pearce et al. (1984); (f) Nb/Rb ‘vs’ Ta/Rb. Errors are 2 s.d. calculated using replicate analyses of MPI-DING StHs6/80 glass. Where not shown errors are smaller than the symbol size.

Figure 5: Major element plots for distinguishing tephra sourced within the Neapolitan volcanic district (Somma-Vesuvius, Campi Flegrei, Ischia). Also shown is the Schiava pumice glass composition. Errors are 2 s.d. calculated using replicate analyses of MPI-DING StHs6/80 glass.

Figure 6: Trace element plots for distinguishing tephra sourced within the Neapolitan volcanic district (Somma-Vesuvius, Phlegraean Fields, Ischia). Errors,

calculated as 2 s.d. using replicate analyses of MPI-DING StHs6/80 glass, are smaller than the symbols.

Figure 7: Major element plots for 36-19 ka Somma-Vesuvius tephras. Errors are 2 s.d. calculated using replicate analyses of MPI-DING StHs6/80 glass. Error bars are not shown where error is smaller than symbols.

Figure 8: Trace element plots for 36-19 ka Somma-Vesuvius tephras. Errors, calculated as 2 s.d. using replicate analyses of MPI-DING StHs6/80 glass, are smaller than the symbols.

Table

	Tectonic setting	Country	Region	Source volcano	Eruption	Marker layer	Dating method	Age (95% prob.) ka BP	Glass data reference	Reference for age
Atlantic	Anorogenic	Portugal	Azores	Terceira	Lajes-Angra Ig.		$^{14}C^{*}$	25.481 ± 0.207	This study	Gertisser et al., 2010
					Linhares-Matela Ig.		$^{14}C^{*}$	41.961 ± 6.411	This study	Gertisser et al., 2010
					Vila Nova-Fanal Ig.		Ar/Ar	50 ± 10, 58 ± 20	This study	Gertisser et al., 2010
					Caldeira-Castelinho Ig.		Ar/Ar	71 ± 4, 83 ± 18	This study	Gertisser et al., 2010
	Anorogenic	Iceland	-	Katla	Solheimar Ig.				Tomlinson et al., 2012c	
	Anorogenic	Iceland	-	Tindfjallajokull	Thorsmork Ig.				Tomlinson et al., 2010	
Central Mediterranean	Post-subduction	Italy	Roman (Latium) Province	Colli Albani	AH04		Ar/Ar	40 ± 6	Cross et al., 2014	Gaeta et al., 2011
					Pepperino Albano (AH05)		Ar/Ar	36 ± 2	Cross et al., 2014	Gaeta et al., 2011
					AH06		relative varve age, LGdM	~35	Cross et al., 2014	Cross et al., 2014
					AH07		Ar/Ar	33 ± 4	Cross et al., 2014	Gaeta et al., 2011
	Post-subduction	Italy	Neapolitan volcanic area	Somma-Vesuvius	Avellino		$^{14}C^{*}$	3.934 ± 0.026	This study	Sevink et al., 2011
					Mercato		$^{14}C^{*}$	8.536 ± 0.091	This study	Zanchetta et al., 2011
					Verdoline		$^{14}C^{\$}$	19.226 ± 0.104	This study	Siani et al., 2004
					Pomici di Base		$^{14}C^{\$}$	22.081 ± 0.173	This study	Siani et al., 2004
	Post-subduction	Italy	Neapolitan volcanic area	Uncertian	Codola		$^{14}C^{\$}$	29.250 ± 0.480	This study	Alessio et al., 1974
					Schiava		stratigraphic position	~36	This study	Giaccio et al., 2008
	Post-subduction	Italy	Neapolitan volcanic area	Campi Flegrei	Agnano Monte Spina		$^{14}C^{*}$	4.514-4.417	Smith et al., 2011	Smith et al., 2011a
					Pomici Principali	C-1	$^{14}C^{\$}$	11.999 ± 0.52	Smith et al. 2011; Tomlinson et al., 2012b	Smith et al., 2011a
					Neapolitan Yellow Tuff	C-2	Ar/Ar & $^{14}C^{\$}$	14.940 ± 1.00 14.194 ± 1.70	Tomlinson et al., 2012b	Deino et al., 2004; Siani et al., 2004
					PRa		Ar/Ar	16.1 ± 0.2	Tomlinson et al., 2012b	Pappalardo et al., 1999
					VRb		Ar/Ar	~28	Tomlinson et al., 2012b	Pappalardo et al., 1999
					VRa		Ar/Ar	30.3 ± 0.2	Tomlinson et al., 2012b	Pappalardo et al., 1999
					TLo				Tomlinson et al., 2012b	
					Campanian Ig.	Y-5, C-13	Ar/Ar & $^{14}C^{\$}$	39.280 ± 0.55 38.950 ± 2.70	Tomlinson et al., 2012b	De Vivo et al., 2001; Wood et al., 2012
					TLf				Tomlinson et al., 2012b	
					TLc				Tomlinson et al., 2012b	
					Tla		Ar/Ar	58.9 ± 1.8	Tomlinson et al., 2012b	Pappalardo et al., 1999
	Post-subduction	Italy	Neapolitan volcanic area	Ischia	Sant Angelo (younger)		K/Ar	20	This study	Civetta et al., 1991
					Sant Montano		K/Ar	34	This study	Civetta et al., 1991
					Agnone		K/Ar	43	Tomlinson et al., accepted	Civetta et al., 1991
					Pietre Rosse		relative varve age, LGdM	45 ± 6	Tomlinson et al., accepted	Tomlinson et al., accepted
					Schiappone		relative varve age, LGdM	50.6 ± 2.0	Tomlinson et al., accepted	Tomlinson et al., accepted
					Monte Epomeo Green Tuff	Y-7, C-18	Ar/Ar	55 ± 2	Tomlinson et al., accepted	Watts et al., 1996

					Porticello		relative varve age, LGdM	59 ± 2	Tomlinson et al., accepted	Tomlinson et al., accepted
					Tisichiello		relative varve age, LGdM	76 ± 3	Tomlinson et al., accepted	Tomlinson et al., accepted
					Olummo				Tomlinson et al., accepted	
					Sant' Angelo				Tomlinson et al., accepted	
	Subduction	Italy	Aeolian arc	Lipari	Monte Pilato		^{14}C*	1.070-1.270	Albert PhD data	Keller, 2002
	Subduction	Italy	Aeolian arc	Stromboli	Secche di Lazzaro		unpublished ^{14}C	~5	Albert PhD data	Petrone et al., 2009
	Subduction	Italy	Aeolian arc	Vulcano	Palizzi A		stratigraphic position	<5.5	Albert PhD data	Frazetta et al., 1983
					Quadrara		$^{230}Th/^{232}Th$	21 ± 3.4	Albert PhD data	Zanella et al., 2001
	Subduction	Italy	Aeolian arc	Salina	Lower Pollara		^{14}C*	26.480-27.770	Albert PhD data	Morche, 1998, Albert et al., 2012
					Grey Porri Tuff				Albert PhD data	
	Anorogenic	Italy	Sicily	Etna	Biancavilla Ig.s	Y1	^{14}C*	17.335 ± 1.39	Albert et al., 2013	Albert et al., 2013
					Giarre D2a		^{14}C*	18.275 ± 0.225	Albert et al., 2013	Coltelli et al., 2000; Albert et al., 2013
					Giarre D1a		^{14}C*	18.685 ± 0.135	Albert et al., 2013	Coltelli et al., 2000; Albert et al., 2013
					D2a Acireale				Albert et al., 2013	
					D1b Acireale		relative varve age, LGdM	19.502 ± 0.302	Albert et al., 2013	Wulf et al., 2008; Albert et al., 2013
	Anorogenic	Italy	Straight of Sicily	Pantelleria	Green Tuff	Y-6	Ar/Ar	45.700 ± 5.00	This study, Jordan PhD data	Scailet et al., 2013
					Mordomo				Jordan PhD data	
					Acqua				Jordan PhD data	
					Cinque Denti				Jordan PhD data	
Eastern Mediterranean	Subduction	Greece	Aegean arc	Nisyros	Upper Pumice		stratigraphic position	>50.4	Tomlinson et al., 2012a	Karkanas et al., this volume
					Lower Pumice				Tomlinson et al., 2012a	
	Subduction	Greece	Aegean arc	Santorini	Minoan	Z-2	^{14}C*	3.588 ± 0.025	This study	Manning et al. 2006
					Cape Riva	Y-2	$^{14}C^{\$}$	22.024 ± 3.21	This study	Fabbro et al., 2013
					Upper Scoriae 2		Ar/Ar	~54 ± 3	This study	Druitt et al. 1999
					Upper Scoriae 1				This study	
					Vourvolous		K/Ar	<100	This study	Druitt et al. 1999
	Post-subduction	Turkey	Western Anatolia	Gölcük	Cycle III eruptions		K/Ar	24 ± 2 to 72.7 ± 4.7	This study	Platevoet et al., 2008
	Subduction	Turkey	Central Anatolia	Acigöl	Güneydağ		U-Th/He	23.8 ± 2.1	This study	Schmitt et al., 2011
					Korudağ		U-Th/He	24.9 ± 2.1	This study	Schmitt et al., 2011
	Subduction	Turkey	Central Anatolia	Erciyes Dağı	Dikkartın		^{36}Cl cosmogenic	10.2 to 7.9	This study	Sarikaya et al., 2006
					Perikartın		^{36}Cl cosmogenic	10.2 to 7.9	This study	Sarikaya et al., 2006
					Karagüllü		^{36}Cl cosmogenic	10.2 to 7.9	This study	Sarikaya et al., 2006

Table

Eruption	Age (95% prob.) ka BP	Locality	Deposit description	Sample	Phenocrysts	Sample description
Avellino	3.934 ± 0.026[1]*	Terzigno Quarry, also known as Vitiello quarry and Pozzelle	60 cm unit of ash and lapilli, and occasional accretionary lapilli	7	San, cpx, amp, grt (plag, ne)	White vesicular pumice and ash.
Mercato	8.536 ± 0.091[2]*	Terzigno Quarry, also known as Vitiello quarry and Pozzelle	Fallout at base is comprised of dense blocks. This fallout unit becomes coarser but interrupted by fine ash layers. Overlain a poorly sorted, massive PDC deposit that is a few metres thick.	4 (fallout at base), 5 (PDC; mid), 6 (PDC; top)	San, cpx, amp, grt (sub-aphyric)	Dense pumice blocks and ash
Verdoline	19.226±0.104[3$]	NE slope of Vesuvius	2 m of alternating lapilli pumice and ash fall beds containing a mix of pumice and scoria throughout. Some interbedded pyroclastic density current deposits.	Top, KP116, KP115, KP114, KP113[$]	San, amp, plag, bt, cpx	Light coloured, highly vesicular to brown/green and grey poorly vesicular scoria
Pomici di Base	22.081±0.173[3$]	Iervolino Quarry, E of Somma Vesuvius	6 m Plinian fall deposit. White pumice dominates at base and the unit grades into black scoria at top (lower member). Overlain by ash and lapilli fall (upper member).	SM20, SM21, SM22, SM23, SM26, SM28[§]	San, cpx, amp, plag, (plag, bt microlites)	Clear pumice with highly vesicular matrix (ca. 80 %) transitioning to brown, microlite-rich scoria, moderately vesicular (ca. 50 %)
Codola	30.680±0.780[4$]	Bosagro Quarry, Quindici Valley Sarno, Santa Lucia	0.7m deposit of alternating brownish ash and pumice lapilli fall. The lower pumice lapilli fall unit consists of light and dark pumice, and the upper fall is comprised of grey scoria.	ZS2002-4, ZS2002-2, ZS2002-1, ZS9736*	San, plag, cpx, bt (amp, ol)	Yellow pumice and grey scoria with some banded clasts. Highly to moderately vesicular.
Schiava	~36[5]	Schiava	0.5 m deposit of alternating ash and white pumice lapilli layers	AS96309*	San, bt, cpx,	White, highly vesicular pumice with fine vesicles

Table

	Campi Flegrei	Ischia	Somma-Vesuvius
Campi Flegrei		Ischia tephra is distinct from post-CI Campi Flegrei tephra, but there is minor overlap between Ischia and the >39 ka Pre-CI/CI Campi Flegrei tephra at low CaO (CaO < 1.8 wt%) and high Na_2O	Campi Flegrei tephra overlap partially with phase 1 Somma-Vesuvius tephra and significantly with phase 2 Somma-Vesuvius tephra in most major and trace elements. Potentially important for post-CI Campi Flegrei tephra which overlap with phase 1 Somma-Vesuvius glasses in age
Ischia	SiO_2 'vs' CaO (Fig. 5b) Na_2O/K_2O 'vs' CaO (Fig. 5c) Zr/Sr 'vs' Th (Fig. 6a) Y 'vs' Th (Fig. 6c)		Ischia tephra are clearly distinguished from tephra from Somma-Vesuvius on most major and trace element plots
Somma-Vesuvius	CaO 'vs' MgO (Fig. 5d) Ta/Th 'vs' Nb/Th (Fig. 6b)	CaO 'vs' SiO_2 (Fig. 5b) MgO 'vs' CaO (Fig. 5d) Zr/Sr 'vs' Th (Fig 6a)	

Table

Eruption	Avellino	Avellino	Mercato	Pomici di Base	Pomici di Base	Verdoline	Codola	Schiava
Source	Phase 2	Phase 2	Phase 2	Phase 1	Phase 1	Phase 1	Uncertian	Uncertian
Analysis	Avellino 7-9	Avellino 7-13	Mercato top 6-31	SM21-6	SM28-28	KP113-11	ZS2002/2 -7	AS9630-1
SiO2	55.10	59.60	60.16	55.20	61.94	60.20	58.24	66.45
TiO2	0.23	0.36	0.24	0.45	0.29	0.36	0.52	0.25
Al2O3	22.50	20.67	20.61	20.35	18.96	19.55	19.76	17.10
FeOt	2.31	2.17	2.14	4.87	3.24	3.46	3.49	1.79
MnO	0.16	0.16	0.16	0.14	0.14	0.16	0.08	0.10
MgO	0.15	0.18	0.15	1.20	0.34	0.22	0.49	0.17
CaO	2.49	2.99	2.29	9.25	3.07	3.03	5.09	2.22
Na2O	7.87	5.38	5.49	3.01	3.91	4.42	3.10	4.23
K2O	9.19	8.51	8.75	5.53	8.11	8.62	9.22	7.02
Rb	596	344	553	195	240	441	282	465
Sr	181	851	75	1560	968	501	1105	154
Y	8.9	7.1	15	20	30	34	29	26
Zr	644	277	769	170	321	382	295	4001
Nb	132	46	104	27	46	63	61	63
Ba	292	969	60	1534	1527	404	1505	74
La	89	46	100	45	67	79	72	95
Ce	160	73	176	89	121	152	127	147
Pr	14	6.5	15.5	9.6	13.5	16.1	15.0	13.2
Nd	39	18	44	37	51	60	57	43.
Sm	4.2	<LOD	<LOD	7.2	9.2	10.0	11.5	6.5
Eu	0.8	<LOD	<LOD	2.0	2.4	2.1	2.3	<LOD
Gd	2.5	<LOD	<LOD	5.8	7.1	7.6	7.7	5.4
Dy	1.6	<LOD	2.1	4.0	5.6	6.2	5.6	4.1
Er	0.9	<LOD	1.2	1.8	3.0	3.3	2.7	2.4
Yb	0.9	<LOD	<LOD	1.9	2.9	3.7	2.4	3.8
Lu	<LOD	<LOD	<LOD	0.3	0.4	0.5	0.3	9.8
Ta	3.3	1.4	2.6	1.4	2.5	3.5	3.1	2.2
Th	83	28	80	15	26	35	26	57
U	35.5	12.8	34.3	4.9	8.2	12.4	6.8	19.4

Figure
Click here to download high resolution image

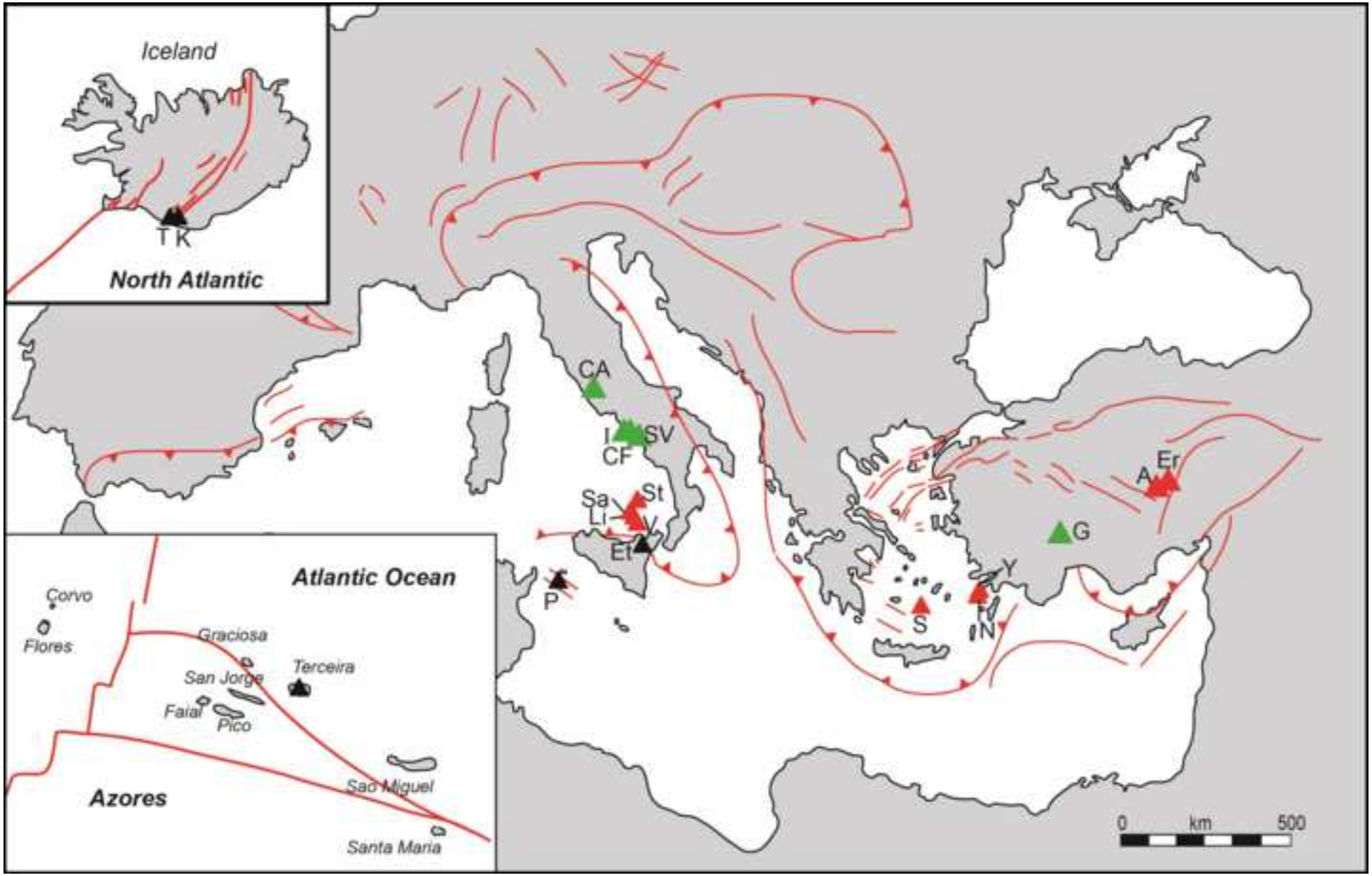

Figure
Click here to download high resolution image

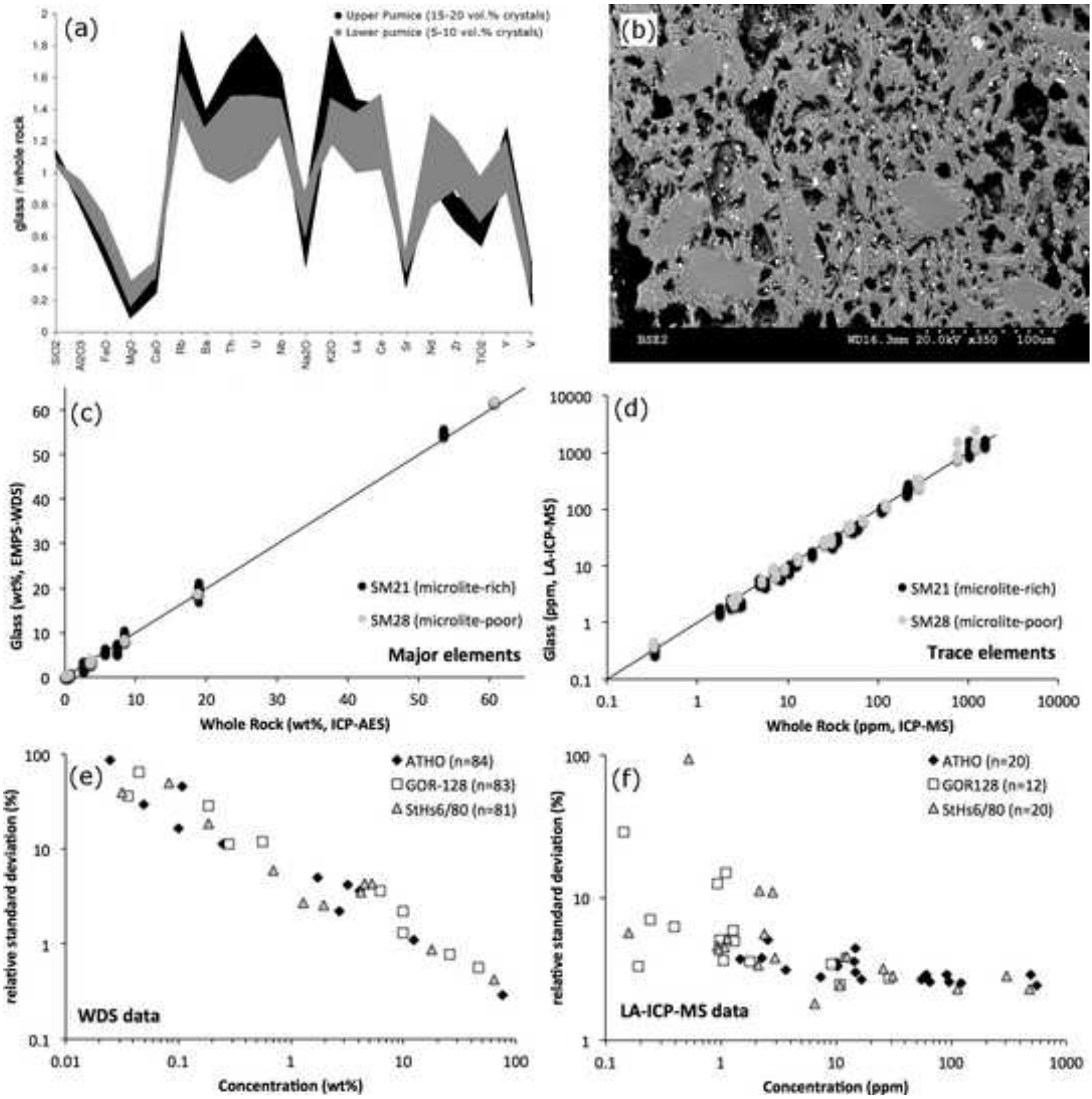

Figure
[Click here to download high resolution image]

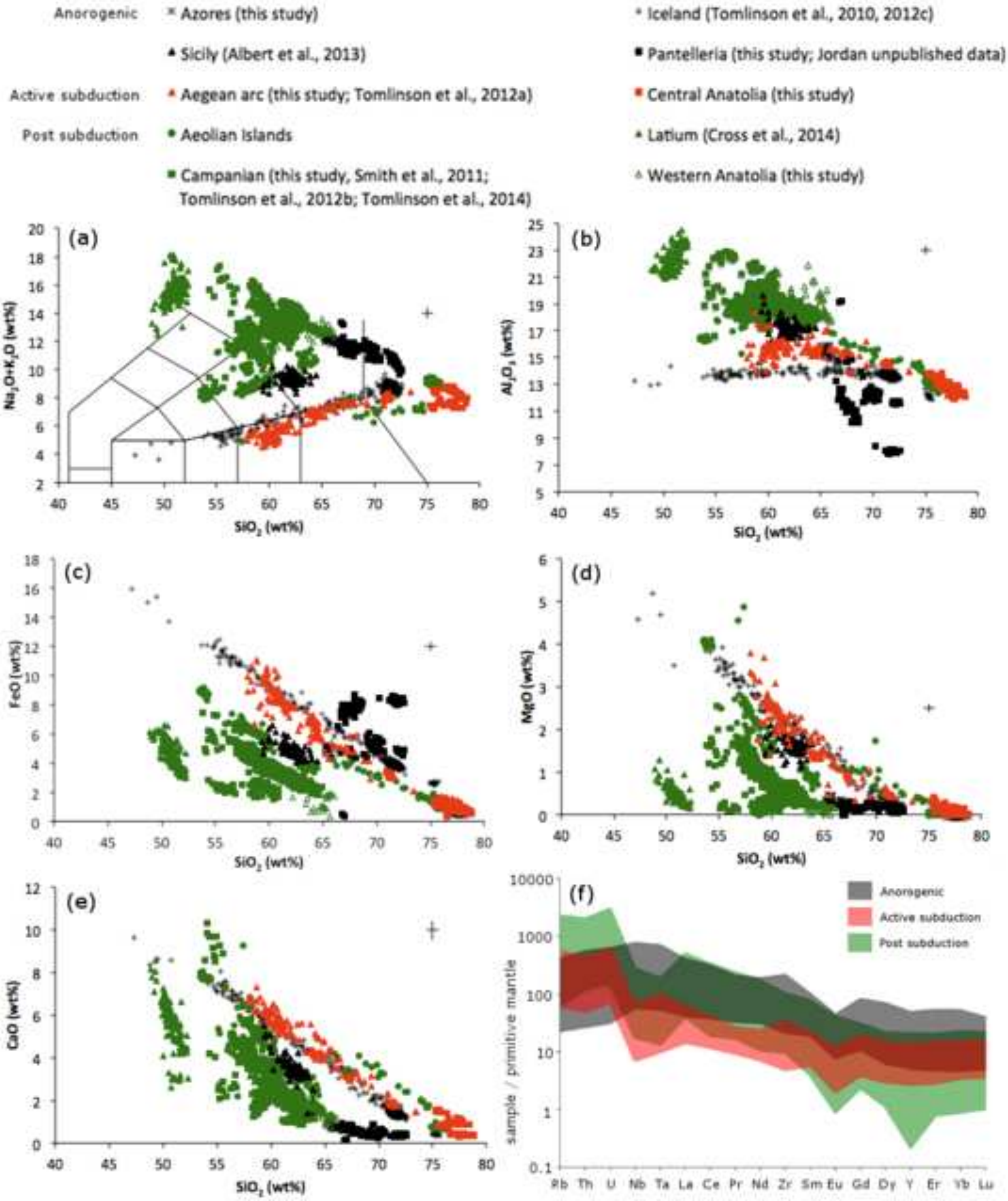

Figure
Click here to download high resolution image

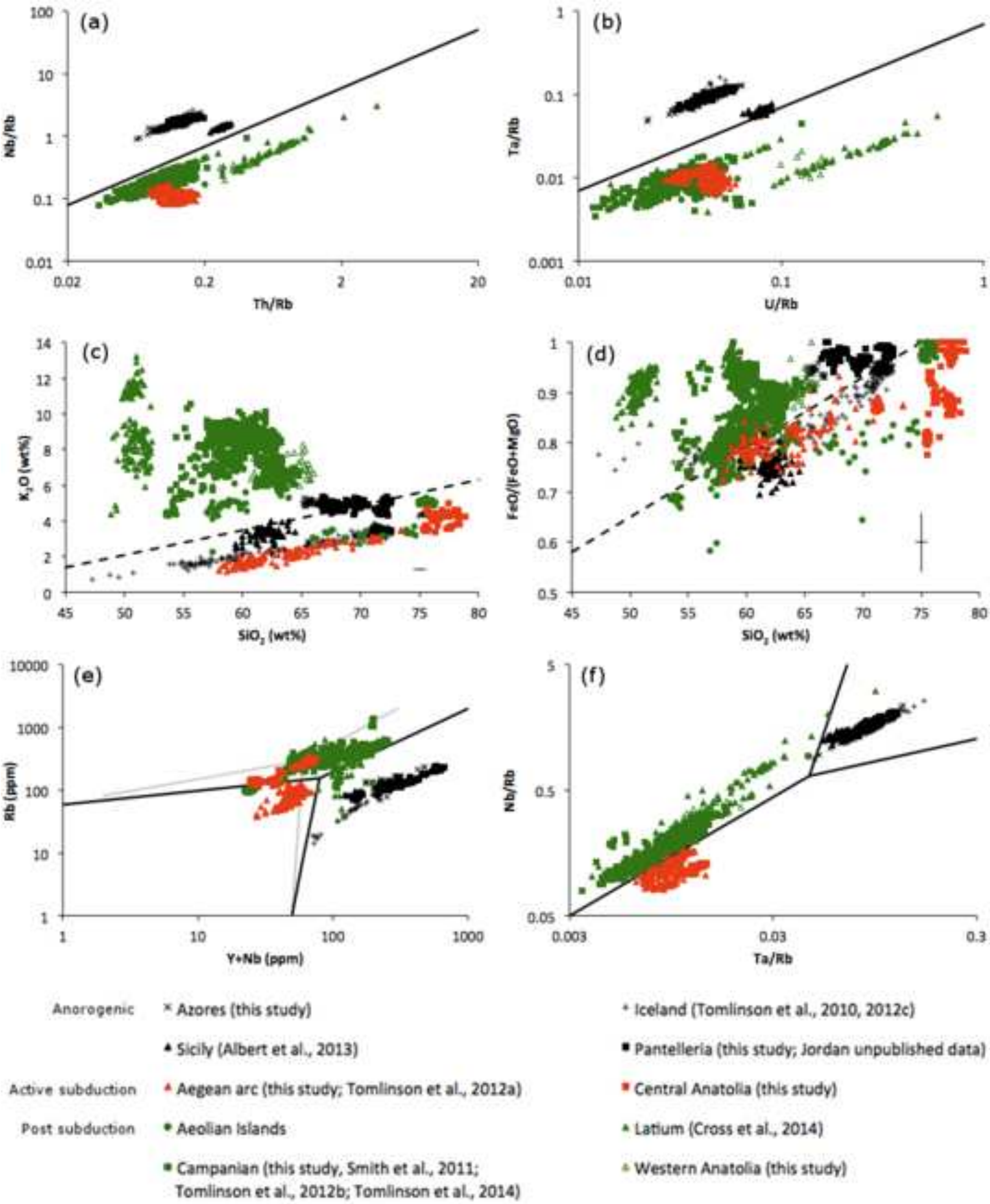

Figure
Click here to download high resolution image

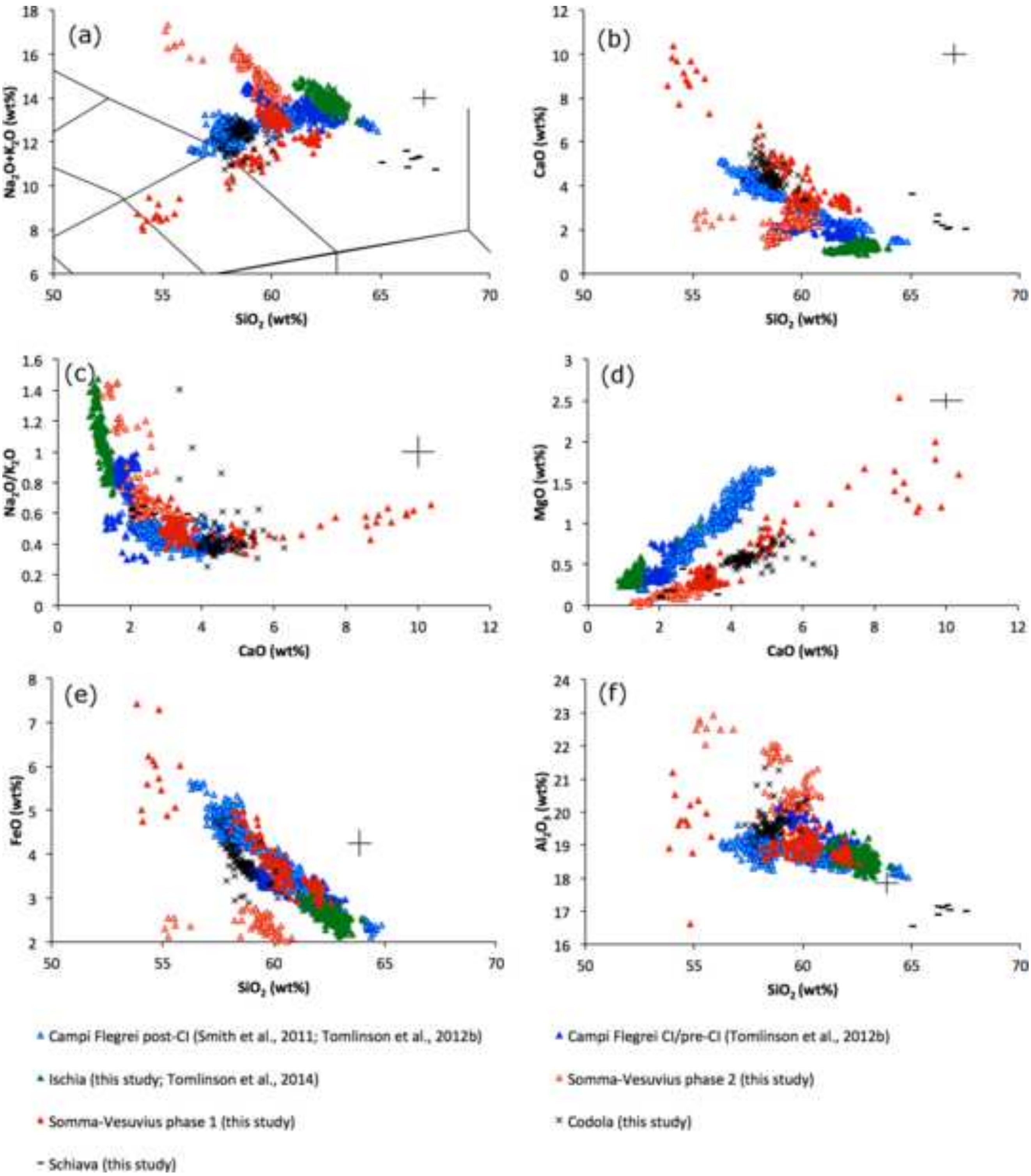

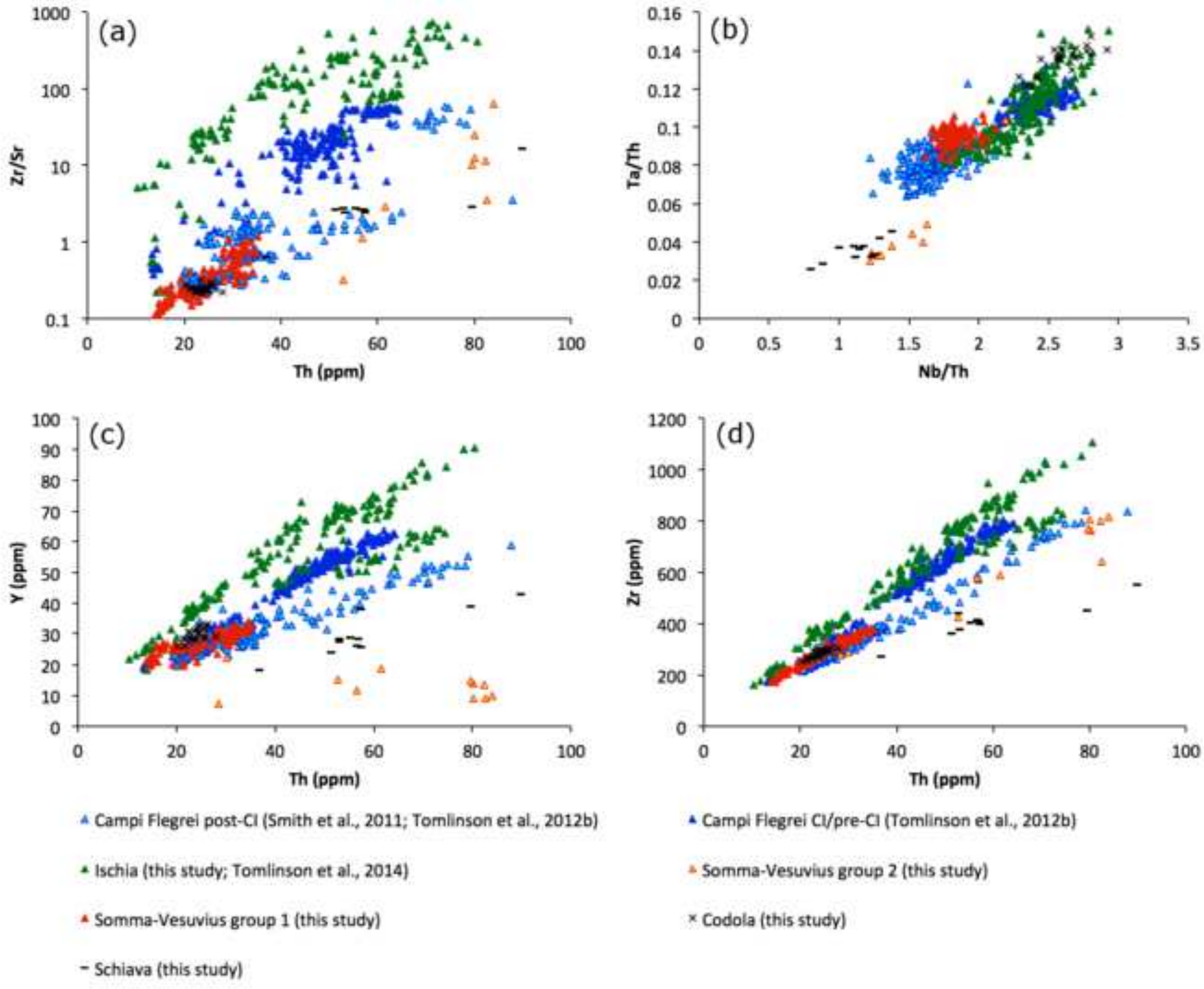
(a)
Zr/Sr
1000
100
10
1
0.1
0
20
40
60
80
100
Th (ppm)
(b)
Ta/Th
0.16
0.14
0.12
0.1
0.08
0.06
0.04
0.02
0
0
0.5
1
1.5
2
2.5
3
3.5
Nb/Th
(c)
Y (ppm)
100
90
80
70
60
50
40
30
20
10
0
0
20
40
60
80
100
Th (ppm)
(d)
Zr (ppm)
1200
1000
800
600
400
200
0
0
20
40
60
80
100
Th (ppm)
Campi Flegrei post-CI (Smith et al., 2011; Tomlinson et al., 2012b)
Ischia (this study; Tomlinson et al., 2014)
Somma-Vesuvius group 1 (this study)
Schiava (this study)
Campi Flegrei CI/pre-CI (Tomlinson et al., 2012b)
Somma-Vesuvius group 2 (this study)
Codola (this study)

Figure
Click here to download high resolution image

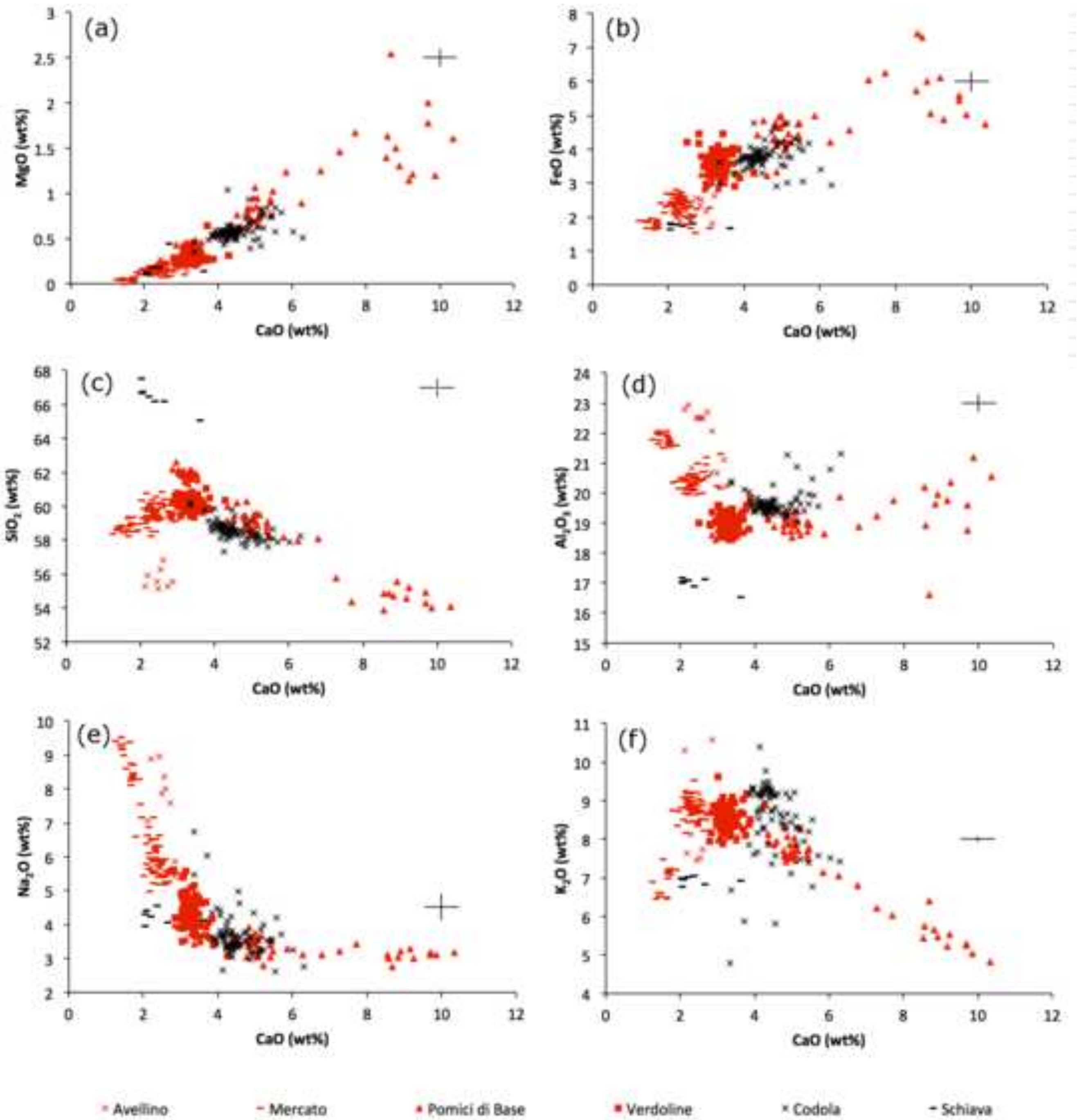

Figure
Click here to download high resolution image

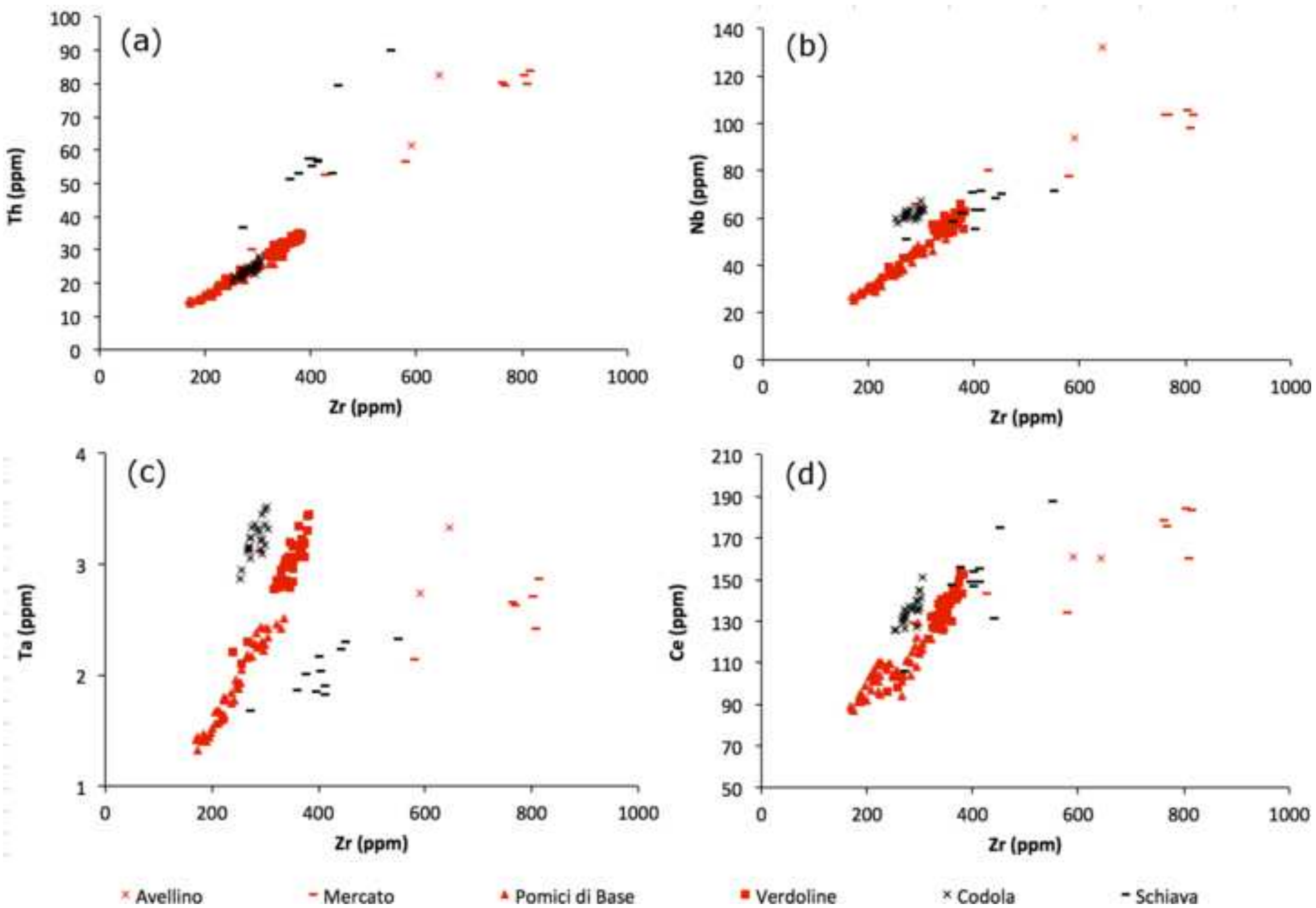

Supplementary Data

Click here to download Supplementary Data: S1_Analytical Methods.docx

Supplementary Data
Click here to download Supplementary Data: S2_Tomlinson.xlsx